



HAL
open science

Revisiting two local constraints of the Galactic chemical evolution

Misha Haywood

► **To cite this version:**

Misha Haywood. Revisiting two local constraints of the Galactic chemical evolution. Monthly Notices of the Royal Astronomical Society, 2006, 371, pp.1760-1776. hal-03733293

HAL Id: hal-03733293

<https://hal.science/hal-03733293v1>

Submitted on 29 Jul 2022

HAL is a multi-disciplinary open access archive for the deposit and dissemination of scientific research documents, whether they are published or not. The documents may come from teaching and research institutions in France or abroad, or from public or private research centers.

L'archive ouverte pluridisciplinaire **HAL**, est destinée au dépôt et à la diffusion de documents scientifiques de niveau recherche, publiés ou non, émanant des établissements d'enseignement et de recherche français ou étrangers, des laboratoires publics ou privés.

Revisiting two local constraints of the Galactic chemical evolution

M. Haywood[★]

GEPI, Observatoire de Paris, F-92195 Meudon Cedex, France

Accepted 2006 July 13. Received 2006 July 12; in original form 2006 April 26

ABSTRACT

I review the uncertainties in two observational local constraints of the Galactic disc chemical evolution: the metallicity distribution of long-lived dwarfs and the age–metallicity relation. Analysing most recent data, it is shown first that the observed metallicity distribution at solar galactocentric radius, designed with standard methods, is more fit to a closed-box model than to the infall metallicity distribution. We argue that this is due to the specific contribution of the thick-disc population, which has been overlooked both in the derivation of the observed metallicity distribution and in the standard chemical evolution models. Although this agreement disqualifies the metallicity distribution as the best supportive (indirect) evidence for infall, we argue that the evolution must be more complex than described by either the closed-box or the standard infall models.

It is then shown that recent determinations of the age–metallicity distribution (AMD) from large Strömgren photometric surveys are dominated by noise resulting from systematic biases in metallicities and effective temperatures. These biases are evaluated and a new AMD is obtained, where particularities of the previous determinations are phased out. The new age–metallicity relation shows a mean increase limited to about a factor of 2 in Z over the disc age. It is shown that below 3 Gyr, the dispersion in metallicity is about 0.1 dex, which, given the observational uncertainties in the derived metallicities, is compatible with the small cosmic dispersion measured on the interstellar medium and meteoritic pre-solar dust grains. A population that is progressively older and more metal rich arises at a metallicity greater than that of the Hyades, to reach $[\text{Fe}/\text{H}] \approx +0.5$ dex at ages greater than 5 Gyr. We suggest that this is best explained by radial migration. A symmetrical widening of the metallicity interval towards lower values is seen at about the same age, which is attributed to a similar cause. Finally, the new derived ages are sufficiently consistent that an age–metallicity relation within the thick disc is confirmed. These new features altogether draw a picture of the chemical evolution in the solar neighbourhood where dynamical effects and complexity in the AMD dominate, rather than a generalized high dispersion at all ages.

Key words: Galaxy: abundances – Galaxy: evolution – solar neighbourhood.

1 INTRODUCTION

The metallicity distribution of long-lived dwarfs and the age–metallicity relation are two often-quoted constraints of the chemical evolution of the Galactic disc: the latter constraint is considered to be weak, whereas the former one is considered to be a strong, or even the ‘strongest’ constraint. Both conclusions are usually perceived as definitive¹ observational results. On the first point, this

is illustrated by the vast majority of papers published in the last decade on the chemical evolution of the Galactic disc, which is described similarly with prolonged infall controlling its progressive inside-out formation. The main motivation for adopting infall being the capacity to reduce the number of metal-poor stars born at early ages, providing a solution to the so-called ‘G dwarf’ problem. How robust is the observational basis – the dwarf metallicity distribution – of such uniformity in models? The unbiased metallicity distribution of dwarfs is usually obtained by weighting the metallicity bins of local samples using a relation between metallicity and the vertical velocity dispersion (σ_w) as measured on these same samples. Due to the small statistics in the lower metallicity bins and the uncertainties that plague the photometric metallicity scales, this process leads to large uncertainties in the level of corrections that are applied, as can be testified by the variety of $[\text{Fe}/\text{H}]$ – σ_w relations found in the

[★]E-mail: Misha.Haywood@obspm.fr

¹In a recent paper on modelling of the chemical evolution of the Milky Way, the authors (Romano et al. 2005) argued that ‘the uncertainties in the data have become really small’ to focus on theoretical uncertainties. A similar conclusion is reached by Nordström et al. (2004) on the ‘G dwarf problem’.

literature (see Fig. 3). The recent release of large catalogues of solar neighbourhood stars (Nordström et al. 2004; Valenti & Fischer 2005) containing radial velocities should significantly improve the situation. The level that this relation should reach at $[\text{Fe}/\text{H}] < -0.4$ dex is usually not questioned (with the exception of Sommer-Larsen 1991); however, it is shown here that the inclusion of the thick-disc stars introduces significant modifications to the diagnostic of the ‘G dwarf problem’. After having questioned the metallicity scales in Haywood (2001, 2002), we point here to the ambiguity caused by the thick-disc population, which, if included in local samples, makes the observed distribution compliant with the predictions of the simple closed-box model. This suggests that some caution should be exercised as long as most of the evidence for prolonged infall is limited to the so-called ‘G dwarf problem’.

Since Edvardsson et al. (1993), the age–metallicity distribution (AMD) is often commented as being highly dispersed at all ages, providing a poor constraint to chemical evolution models of the Galaxy. Two recent studies, based on large photometric data sets, have claimed a similar result (Feltzing, Holmberg & Hurlley 2001; Nordström et al. 2004). However, and though it has received little attention (but see Pont & Eyer 2004), these recent AMDs illustrate a rather atypical chemical evolution, where the youngest stars (<3 Gyr) show the largest range of metallicities, stars between 5 and 10 Gyr show negative evolution (i.e. mean decreasing metallicity with age), and the lowest-metallicity stars ($[\text{Fe}/\text{H}] < -0.5$) are more often ‘young’ (age <5 Gyr) than old. Although such non-conventional evolution is not excluded [one can think of an enhanced infall episode increasing the dilution of metals in the interstellar medium (ISM)], confirmation is needed. Moreover, the large dispersion at all ages is difficult to reconcile with the very small dispersion that is measured either in the local ISM (Cartledge et al. 2006), on meteoritic pre-solar grains (Nittler 2005), or abundance ratios, which all suggest that the gas from which stars are born is very homogeneous at all times in the disc, the thick disc, and probably the halo (Arnone et al. 2005).

In the following section, we present a discussion of recent metallicity distributions and scaleheight corrections, while the third section focuses on the biases in the age–metallicity relation. Section 4 presents a derivation of a corrected AMD, which although not optimized, is quite different from the previously cited studies. We conclude in Section 5.

2 THE METALLICITY DISTRIBUTION

We first review the metallicity scales used in recently published studies of the local metallicity distribution, and then focus on the scaleheight corrections.

2.1 Photometric metallicity scales

In discussing the local metallicity distribution, the value at which this distribution peaks is a key issue, related to the thick disc. In a closed-box model centred on solar metallicity, the percentage of material which forms between $[\text{Fe}/\text{H}] = -1.0$ and -0.50 is about 18–20 per cent. Allowing for a thick disc with about 5–8 per cent of the local stellar density and a scaleheight of about 800–1000 pc, we arrive at a percentage of 16–21 per cent of the total stellar surface density (assuming 250 pc scaleheight for the thin disc). Given the uncertainties in these parameters, the two estimates can be considered as compatible. If the observed peak was at $[\text{Fe}/\text{H}] = -0.2$ dex or lower, the predicted percentage of stars between $-1.0 < [\text{Fe}/\text{H}] < -0.5$ in a closed-box model centred on this value

(-0.2 dex) would be higher than ≈ 30 per cent, a value incompatible with the thick-disc characteristics. The thick-disc and photometric metallicity scales are therefore at the centre of the discussion about the mean metallicity of the solar neighbourhood stars, but the literature published on the subject since 1989 shows this mean has a high variability. The mode of the metallicity distribution of long-lived dwarfs in the solar neighbourhood has fluctuated between -0.4 dex (Pagel 1989) and -0.05 dex (Haywood 2001), with intermediate values by Wyse & Gilmore (1995), Rocha-Pinto & Maciel (1996), Kotoneva et al. (2002b) and Jørgensen (2000). This is somewhat surprising since, for example, over the same period, the same quantity for halo stars has been left relatively undisputed at ≈ -1.5 dex. One possible reason is that halo stars are often measured spectroscopically, whereas, paradoxically, systematic spectroscopic surveys of nearby disc stars have commenced only very recently (Allende Prieto et al. 2004; Luck & Heiter 2005; Valenti & Fischer 2005), impeded, in particular, by planet-search programmes.

Since Haywood (2001), a few studies relevant to the ‘G dwarf problem’ have been published, in particular from Kotoneva et al. (2002b), and the spectroscopic complete surveys just mentioned. The metallicity scale by Kotoneva et al. (2002b) differs from ours by a significant amount (0.2 dex), and we go here into some detail explaining the origin of this difference, and then we compare with spectroscopic surveys.

2.1.1 Kotoneva et al. 2002b

There is a difference of about 0.2 dex between the distribution of Kotoneva et al. (2002b) and that of Haywood (2001). We now try to clarify this point. Kotoneva et al. (2002b) asserted that the calibration used in Haywood (2001) is biased, based on a $(B - V, [\text{Fe}/\text{H}])$ plot (their fig. 8) taken from our sample of long-lived dwarfs (Haywood 2001). However, judging a calibration from a set of selected long-lived dwarfs is strongly misleading, because it shows only stars that are chosen based on their colour being redder than a given isochrone. This process imposes a limit that, varying with metallicities, is colour-dependent. This limit is visible in their fig. 8, where they showed our sample of long-lived stars. It is only an effect of the selection of long-lived dwarfs, not of the metallicity calibration. This is the sense of the ‘bias’ seemingly detected by Kotoneva et al. (2002b) and, which, therefore has nothing to do with a bias in the metallicity calibration we used.

Although their explanation is incorrect, Kotoneva et al. (2002b) conclusively found a discrepancy of about 0.2 dex between their calibration and the one we adopted, evaluated with 104 common stars. What can be the origin of this discrepancy? We have already commented on our metallicity scale in Haywood (2002) and nothing new in Kotoneva et al. (2002b) indicates a possible problem of our calibration (see also a discussion of our results by Taylor & Croxall 2005). Could the problem originate in the metallicity calibration of Kotoneva et al.? Fig. 1 shows the solar metallicity isochrone of Kotoneva et al. (2002b) they took as a reference scale, which difference of absolute magnitude to a given star is used as a metallicity indicator. On the same plot, we also show the Hyades sequence as given by de Bruijne, Hoogerwerf & de Zeeuw (2001), together with a fit representing this sequence. Since the Hyades cluster has a metallicity of $+0.14$ dex, we would expect its sequence to be systematically 0.12 mag above the isochrone (according to the relation between metallicity and the difference in magnitude of Kotoneva et al. 2002a). As can be seen from the plot, this is not the case: the Hyades sequence is systematically *below* the isochrone at $B - V >$

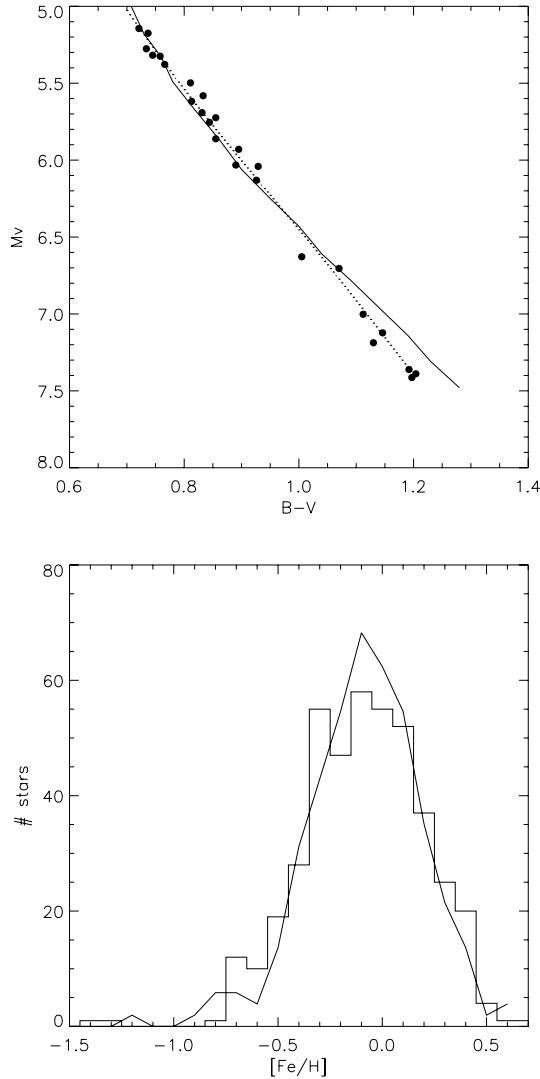


Figure 1. (a) The Hyades sequence from de Bruijne et al. (2001) (black dots), with the solar metallicity isochrone from Kotoneva et al. (2002a). The dotted sequence is a fit to the observed Hyades sequence. At $0.75 < B - V < 1.07$, the isochrone is very close to the Hyades fit, and below it outside these limits. (b) The histogram of the stars selected by Kotoneva et al. (2002b), with the metallicity calculated using the Hyades sequence as the reference (limited to $B - V < 1.3$). It agrees well with the distribution given in Haywood (2002, fig. 6), solid curve.

0.95 and $B - V < 0.75$, and the difference is much less than 0.12 mag between these limits. It means that their isochrone is probably in error, and it follows that the calibration of Kotoneva et al. will systematically underestimate the metallicity of the stars over the whole colour range (by about 0.15 dex), and most severely at $B - V > 1.0$.

Although their solar metallicity isochrone is incorrect when compared to the Hyades sequence, it seems to fit well the Hertzsprung–Russell (HR) diagram of field, ‘calibrating’ stars, selected on the basis of photometrically determined metallicity (fig. 9 of Kotoneva et al. 2002a). How can this be understood? Kotoneva et al. did not fit their isochrone to solar metallicity stars *per se*, but to stars selected to have $0.1 < [\text{Fe}/\text{H}]_{\text{photo}} < 0.3$. The argument assumed by the authors being that, due to observational errors in the determination of

photometric metallicities, and the peaked distribution of metallicities, stars in the metal-rich part of the metallicity distribution (at solar metallicities, in this case) will be contaminated by the lower, dominant metallicities (at $[\text{Fe}/\text{H}] \approx -0.2$ dex, in their study). To correct for this effect, and to select stars which have a metallicity which is truly solar, the authors selected stars showing photometric metallicities in the range $0.1 < [\text{Fe}/\text{H}]_{\text{photo}} < 0.3$. This process meets two difficulties: first, the correction can be safely evaluated *only* if the metallicity distribution is known a priori, which is a dubious method since the metallicity distribution is what they wanted to determine, and secondly, if the solar neighbourhood metallicity distribution peaks at $[\text{Fe}/\text{H}] \approx 0.0$, and not -0.2 dex (and assuming a symmetrical distribution), then the correction to apply when selecting solar metallicity stars is zero. If this is the case (Haywood 2001), it implies that the ‘calibrating’ stars in Kotoneva et al. (2002b) are, in the mean, genuine high-metallicity stars. Unfortunately, very few of the 26 calibrating stars of Kotoneva et al. (2002b) have a spectroscopic metallicity in the catalogue of Cayrel de Strobel, Soubiran & Ralite (2001). However, HIP 99825 has a metallicity of -0.09 dex ($+0.05$, Israelian et al. 2004); HIP 58345 has a metallicity of $+0.16$ dex; HIP 19788 has a metallicity of $+0.04$ dex; HIP 15919 has metallicities of $+0.26$ and $+0.33$ dex; and HIP 74135 has a metallicity of 0.16 dex.

It is also possible to compare the metallicities in the whole catalogue of Kotoneva et al. (2002b) (not only the calibrating stars) with spectroscopic measurements. For the 31 stars in common with the catalogue of Cayrel de Strobel et al. (2001), the mean difference is 0.107 dex, in the sense that Kotoneva et al. (2002b) underestimated the metallicities. Using the newly published data by Kovtyukh, Soubiran & Belik (2004), we found that, for 34 stars in common between these two studies, the mean difference is also at 0.11 dex. Laws et al. (2003) found a similar difference between their spectroscopic values and the metallicities of Kotoneva et al. (2002b). The great majority of these common stars have $B - V < 1.1$. The coincidence between their isochrone and the Hyades sequence in this same colour interval (see Fig. 1) implies a similar mismatch in metallicities. At $B - V > 1.1$, the difference rises to larger values (implying underestimates probably larger than 0.2 dex), their reference isochrone being above the Hyades sequence. As a last check, we have computed the metallicity of the Hyades stars, using the absolute magnitudes derived by de Bruijne et al. (2001) and the calibration by Kotoneva et al. (2002b, equation 4). For the 23 members with $0.8 < B - V < 1.2$, the derived mean metallicity is $+0.045$ dex, while restricting the selection to $0.9 < B - V < 1.2$ (13 members) yields -0.03 dex. This amounts to 0.095- and 0.17-dex differences if the spectroscopic metallicity of the Hyades stars is 0.14 dex, and is consistent with our comments on the metallicities of field stars.

The method adopted by Kotoneva et al. is, however, a useful alternative to classical metallicity indicators in a colour range where metallicity estimates are notoriously difficult. An interesting exercise is to recalculate the metallicities in the sample of Kotoneva et al. (2002b), using the Hyades sequence as the reference sequence. This has been done using ΔM_V calculated for each star with the polynomial fit as the Hyades reference for $B - V < 1.3$ (the limit of our polynomial). The calibration of Kotoneva et al. (2002a) is now modified to

$$[\text{Fe}/\text{H}] = 1.185 \Delta M_V + 0.14.$$

The new metallicity histogram of the star sample of Kotoneva et al. is plotted in Fig. 1(b), and shows that the distribution is now fully compatible with our own result (Haywood 2001).

Finally, Kotoneva et al. (2002b) cited the study of Rocha-Pinto & Maciel (1997) as confirming their results, in contradiction to our work. The study of Rocha-Pinto & Maciel (1997) is based on the calibration of Schuster & Nissen (1989), which, for K dwarfs, is known to produce a strong bias on solar and supersolar metallicity stars, when applied on the Strömgren photometry of Olsen. (see Haywood 2002; Twarog, Anthony-Twarog & Tanner 2002).

2.1.2 Spectroscopic samples

Three different spectroscopic surveys of solar neighbourhood stars have started in the recent years by Allende Prieto et al. (2004), Luck & Heiter (2005) and Valenti & Fischer (2005). There is about 0.10-dex offset between our metallicity distribution and that given in the 15-pc sample of Allende Prieto et al. (2004), in the sense that we give higher metallicities. In contrast, the work of Luck & Heiter (2005) and Valenti & Fischer (2005) agreed well with our own study, with peak in the distributions around $[\text{Fe}/\text{H}] = 0.0$ dex. This is perhaps not surprising, since Allende Prieto et al. (2004) used Strömgren photometry and the calibration of Alonso, Arribas & Martinez-Roger (1996) to derive effective temperatures, which scale is known to be offset by 100–150 K compared to spectroscopic scales (see Section 3.2 below). To summarize, we plot in Fig. 2 the distributions of these different studies, showing that there is a good overall consistency between the spectroscopic surveys (keeping in mind our comment about the Allende Prieto et al. sample) and Haywood (2001). [Note that the sample of Haywood (2001) in Fig. 2 is limited to long-lived dwarfs. However, comparison of the long-lived dwarfs metallicity distribution and the original sample in Haywood (2001) shows that the two distributions peak at the same metallicity.] The shift of about 0.2 dex noted for the Kotoneva et al. (2002b) sample is well in evidence.

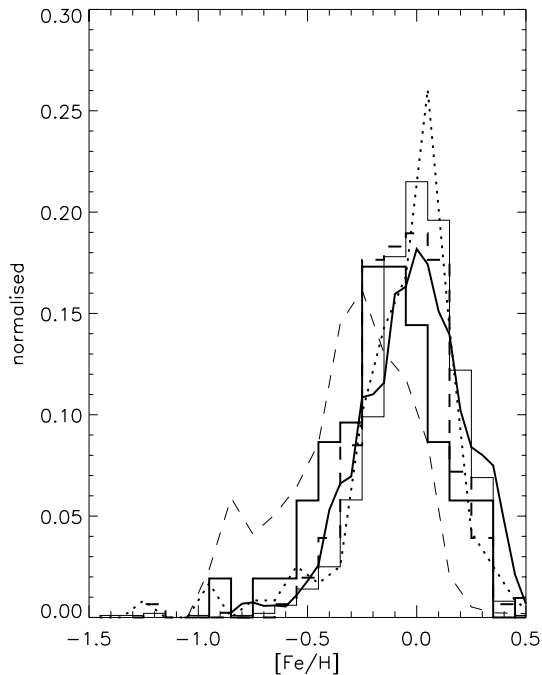


Figure 2. Metallicity distributions for the samples discussed in Section 2. Haywood (2001): thick curve; Kotoneva et al. (2002b): dashed curve; Luck & Heiter: dotted curve; Valenti & Fischer (2005), whole sample: thin line histogram; Valenti & Fischer (2005), 18-pc sample: dashed histogram; and Allende Prieto et al. (2004): thick line histogram.

2.2 Scaleheight corrections

Because old stars make a kinematically hotter component than the young disc, they display a broader vertical density distribution in a given potential. Their Galactic plane density is correlatively lower, and they are under-represented in local samples. This differential (age) effect biases all estimates of the density and must be taken into account. The corrections are usually calculated using a model of the vertical structure of the Galactic disc related to the metallicity distribution through a metallicity–vertical velocity dispersion (σ_w) relation. Fig. 3(a) shows various $[\text{Fe}/\text{H}]$ – σ_w relations used in different studies for correcting the observed distributions. As can be seen, there are wide variations in these scaleheights, the important point being the amplitude between the minimum and maximum of σ_w . Plot (b) shows the corresponding corrections adopted by these studies. The same corresponding large spread is seen, from about 2 for Kotoneva et al. (2002b), and 5 for the option (line 3 in Fig. 3b) proposed by Sommer-Larsen (1991). The result of Kotoneva et al. (2002b) is somewhat surprising, because the thick disc is expected to

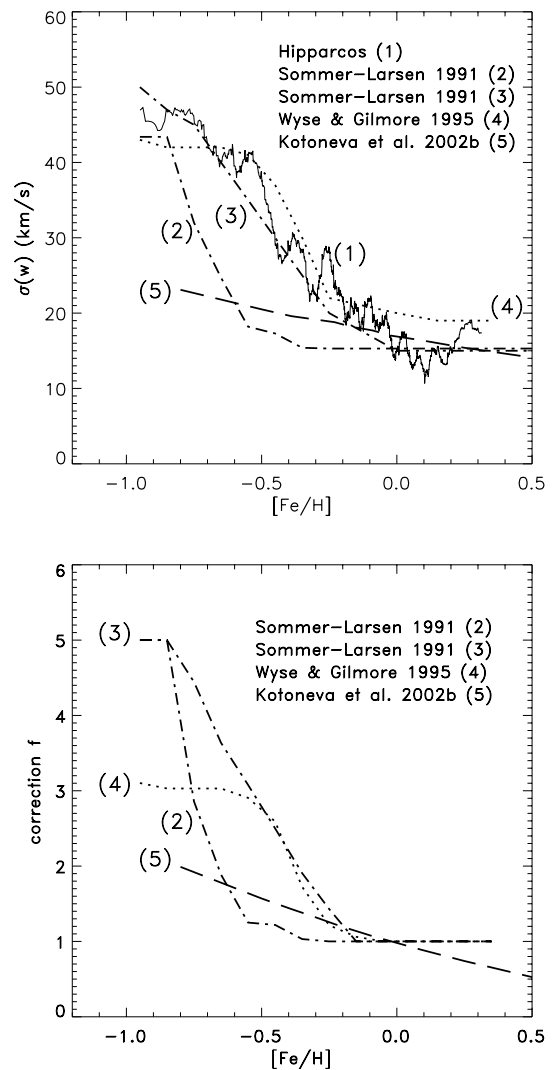


Figure 3. (a) $[\text{Fe}/\text{H}]$ – σ_w relations used in different studies to correct the local metallicity distribution. The black curve is the relation obtained over 3140 stars with metallicity from Geneva photometry and W from Nordström et al. (2004). (b) The corrections for these same studies, normalized at the solar metallicity.

contribute (if not to dominate) at $[\text{Fe}/\text{H}]$ between $[-0.6, -0.8]$ dex, while their σ_w value seems to indicate a pure disc sample.

In Fig. 3(a), we show [labelled *Hipparcos* (1) on the plot] the running dispersion of a sample of 3140 stars with Geneva photometry and well-defined kinematics from the sample of Nordström et al. (2004). Although the sample is not complete in distance, it is sufficiently large that undersampling uncertainties are small, the metal-weak ($[\text{Fe}/\text{H}] < -0.5$) part of the sample representing a fair 9 per cent of the sample. The vertical velocity dispersion decreases from about 46 km s^{-1} to about 13 km s^{-1} at $[\text{Fe}/\text{H}] = 0.1$ dex. The rise at supersolar metallicities is due to the inclusion of old, metal-rich objects. A similar result is obtained with the sample of Soubiran & Girard (2005). Selecting from their sample stars they identified as thin- and thick-disc objects (excluding members of the Hercules stream), the dispersion varies from about 42 km s^{-1} at $[\text{Fe}/\text{H}] < -0.65$ dex to about 13 km s^{-1} between $-0.1 < [\text{Fe}/\text{H}] < +0.1$ dex. These new data clearly illustrate that the largest (NR option in his paper) scaleheight corrections of Sommer-Larsen (1991) are very near to the observed solar neighbourhood metallicity– σ_w relation.

2.3 Comparison with the closed-box model

Having determined the scaleheights, we want to compare the observed and model metallicity distributions. Usually, scaleheight corrections are applied to the observed metallicity distribution. However, due to the small number statistics of our original sample (Haywood 2001) at $[\text{Fe}/\text{H}] < -0.5$ and the uncertainties in the metallicity scale, this procedure will systematically amplify Poisson variations in the observed metallicity distribution. We prefer to bring the model nearer to the observations and apply the scaleheight corrections to the predictions of the closed-box model. Fig. 4 shows the closed-box model prediction, corrected to give volume density distribution and convolved with 0.1-dex Gaussian errors, together with the long-lived dwarf metallicity distribution of Haywood (2001). As is clear from the figure, there is no marked disagreement between the two distributions. There is a slight overestimate of the model at $[\text{Fe}/\text{H}] < -0.5$, but this is hardly significant, given the uncertainties in the detailed profiles of the scaleheight corrections and metallicity scales. It is clear from what has been said that the match between the closed-box model and the observed distribution is satisfactory only because the thick disc has been included in the comparison.

2.4 Discussion

Formally, we have shown that, using the same procedures as those found in studies of the ‘G dwarf problem’ and strictly restricting our case to the fit of the metallicity distribution, the most up-to-date data do not lead to a ‘G dwarf problem’. Before the significance of this ‘no-G dwarf problem’ can be discussed (Section 5), it is important to point out several inconsistencies that have hampered a clear assessment of this question in the last fifteen years or so.

Our result, based on local data, is compatible with arguments of Galactic structure evocated in the introduction section that, given the properties of the thick disc (scaleheight and local density), this population should contribute (at $-1.0 < [\text{Fe}/\text{H}] < -0.5$ dex) a rough 15–20 per cent of the – corrected for volume effect – metallicity distribution. This point is barely discussed in the literature on the subject, and we may ask how the thick-disc contribution is dealt with in the numerous studies published on the subject. In papers deriving the observed metallicity distributions, thick-disc stars are not

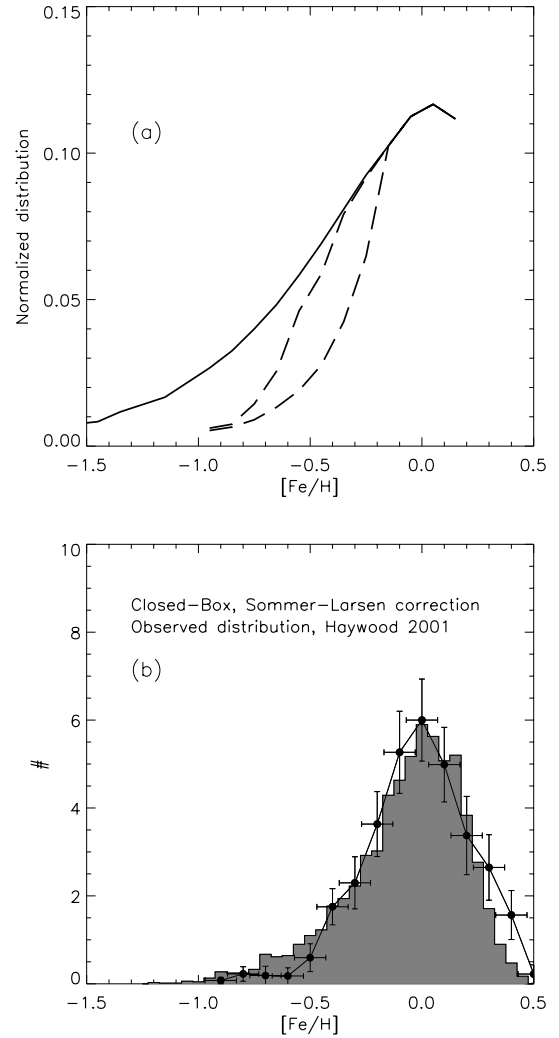


Figure 4. The closed-box model metallicity distribution (continuous curve) and the (local) volume density closed-box model, corrected using the scaleheight corrections of Sommer-Larsen (2) and (3) of Fig. 3.

disregarded and therefore should have significant contribution when volume corrections are considered. However, the characteristics of the derived metallicity distributions do not meet the expectations just mentioned. In the distribution by Jørgensen (2000) (the characteristics of which are the nearest to our own distribution), the contribution of the stars with $-1.0 < [\text{Fe}/\text{H}] < -0.5$ dex is left almost completely unmodified by the scaleheight corrections, representing from about 5 (uncorrected) to 7 per cent (corrected) of the total distribution. In Kotoneva et al. (2002b), and assuming that their metallicity scale has to be moved up by $+0.2$ dex (see Section 2.1.1), the contribution of stars in this same metallicity interval, after correction for volume effect, is only 12 per cent.

In papers where models are designed to fit the observed distribution, the thick disc is usually acknowledged as a genuine Galactic population. In most cases, however, models would not be able to fit both 15–20 per cent of the distribution between $-1.0 < [\text{Fe}/\text{H}] < -0.5$ dex and a peak centred at $[\text{Fe}/\text{H}] = 0.0$ dex. Limiting our census to the most recent models, in Chiappini, Matteucci & Gratton (1997), the percentage of stars within $-1.0 < [\text{Fe}/\text{H}] < -0.5$ dex given by the model is about 12 per cent, and the peak is centred on $[\text{Fe}/\text{H}] = -0.1$ dex. Shifting it to solar metallicity would make the

‘thick disc’ even less conspicuous. Alibés, Labay & Canal (2001) metallicity distribution is similar. In Renda et al. (2005), the material produced by the model within this metallicity range matches the lower thick-disc estimates (16 per cent); however, the peak metallicity is set at $[\text{Fe}/\text{H}] = -0.2$ dex, to comply with the observed distribution of Kotoneva et al. (2002b).

In most (if not all) recent studies of the dwarf metallicity distribution, the thick-disc contribution seems to have been overlooked by both the models and in papers deriving the metallicity distribution from observation.

3 THE AGE–METALLICITY RELATION

The AMD is considered a loose constraint of the Galactic chemical evolution, because of the lack of clear trends and the discrepant results that have been obtained. Suggestions for the existence of such relation have been given by Powell (1972) and Hearnshaw (1972), followed by Twarog (1980), while Carlberg et al. (1985) found a rather flat and dispersed relation. More recent work (Edvardsson et al. 1993) have also cast some doubt on the existence of a clear correlation between age and metallicity. In contrast, a study based on chromospheric activity by Rocha-Pinto et al. (2000) found a rather tight correlation. At the same time, Garnett & Kobulnicky (2000) demonstrated that the large scatter in metallicity in Edvardsson et al. (1993) is more likely to reflect the sample selection than real scatter in the local stars. The overall impression is therefore that the issue has not been settled with pre-*Hipparcos* data. There are good reasons to this failure that were already known to Tinsley (1974), ‘that stars of all ages have a considerable dispersion in Z ’, while ‘the mean value is a very slow increasing function of birth epoch’. The publication of the *Hipparcos* catalogue (1997) and the Geneva–Copenhagen Survey (GCS) (Nordström et al. 2004) have been important milestones for the study of the solar neighbourhood, so that we may ask: did we get closer? Feltzing et al. (2001) and Nordström et al. (2004) have provided the most comprehensive studies, with samples of about 5000 stars or larger and detailed age determinations, pointing to a similarly dispersed AMD. Pont & Eyer (2004) focused on a restricted but careful age determination and discussed a possible correlation in the Edvardsson et al. (1993) sample. Pont & Eyer (2004) have demonstrated that classical isochrone dating method is subject to biases that naturally arise in regions of the HR diagram where the effects of ages on the atmospheric parameters become small, even when the calibration scales providing these atmospheric parameters are correctly set.

We take here a different view, and try to evaluate how ages are affected when such calibrations are biased. We show how explicit biasing of the atmospheric parameters can lead to structures and spurious patterns in the AMD, even at ages below 3 Gyr, and then we focus on analysing the recent AMDs of Feltzing et al. (2001) and Nordström et al. (2004). Although we use mostly the GCS catalogue from Nordström et al. (2004), our conclusions are applicable to Feltzing et al. (2001), since Nordström et al. (2004) have used essentially the same input data and calibrations, and obtained a similar AMD.

3.1 Modelling biases in the AMD

In order to evaluate the effect of systematic and random errors on the determination of age in photometric samples, we apply the following simple procedure. We assume a model AMD, from which we generate a sample of about 10 000 points in the HR diagram,

using a set of isochrones (Yi, Kim & Demarque 2003). The sample of simulated ‘stars’ is limited to absolute magnitude $2 < M_V < 5.5$, and $0.3 < B - V < 1.0$.

Systematic biases and random errors are then introduced on the atmospheric parameters T_{eff} and $[\text{Fe}/\text{H}]$, from which we try to recover the age using the isochrone-fitting method (and the same set of isochrones). We can then compare the resulting ages with the initially assumed relation. Although we test what can be expected from the data only, with no interference from the stellar models, it must be kept in mind that they are a source of uncertainty that is difficult to evaluate. Stellar models certainly can generate similar systematic effects as those studied here, by being too hot, too cold, etc. Also, the test is a simplified one, and does not take into account effects, such as unresolved binaries, α -enrichment of the stellar models, error on absolute magnitude, etc.

The age search is made by scanning a set of isochrones at the metallicity of the star to minimize the χ^2 quantity:

$$\chi^2 = (M_V^o - M_V^m)^2 + 16 (\log T_{\text{eff}}^o - \log T_{\text{eff}}^m)^2, \quad (1)$$

which is the formula introduced by Ng & Bertelli (1998) and also used by Feltzing et al. (2001). The subscript ‘o’ is meant for observations and ‘m’ for model. The model and recovered age–metallicity relations are shown in Fig. 5, assuming different biases on atmospheric parameters, as described below.

(i) We first assume a theoretical AMD, represented by a single curve, with no intrinsic dispersion in metallicity at a given age, no bias on atmospheric parameters. The aim here is to evaluate the uncertainties due to the method. The result is given in Fig. 5(a), and shows that besides a few points at ages smaller than 5 Gyr, due to overlapping isochrones in the hook region, the method is satisfactory. This feature disappears when the hook itself disappears, at ages greater than 5 Gyr.

(ii) The ages are now recovered assuming 0.1 dex and 50 K dispersion in the input metallicities and effective temperatures in order to simulate the effect of a reasonably small observational scatter. The result is given in Fig. 5(b). The curve gives the dispersion in metallicity as a function of age, and shows that there is no increase in the dispersion in metallicity at ages less than 12 Gyr. Only 5 per cent of the stars have a new age differing by more than 0.1 Gyr from their true age; hence, if no other sources of error are present, the determination of the AMD can be made with confidence.

(iii) The AMD have now been biased systematically in temperature and metallicity, while the random errors are the same as previous values (0.1 dex in $[\text{Fe}/\text{H}]$, 50K in T_{eff}). The results are shown in Fig. 6 for various combinations of biases. It can be seen that combining moderate random errors and biases easily produces significant deviations from the original relation, with ages modified by several Gyr (up to almost 10 Gyr in the case of underestimated effective temperatures). Although biases in metallicity affect the shape of the AMD, biases in effective temperature have the most dramatic effects, easily creating young metal-poor or old metal-rich stars with just a hundred-degree bias on effective temperatures. Another consequence is that, starting from an AMD with no intrinsic scatter, a dispersion in metallicity of about 0.15–0.20 dex is easily reached with a combination of (limited) observational random errors and systematic bias on effective temperatures, in particular for old stars. It implies that a combination of even relatively minor systematics on effective temperatures and metallicities can seriously affect the general morphology of the AMD.

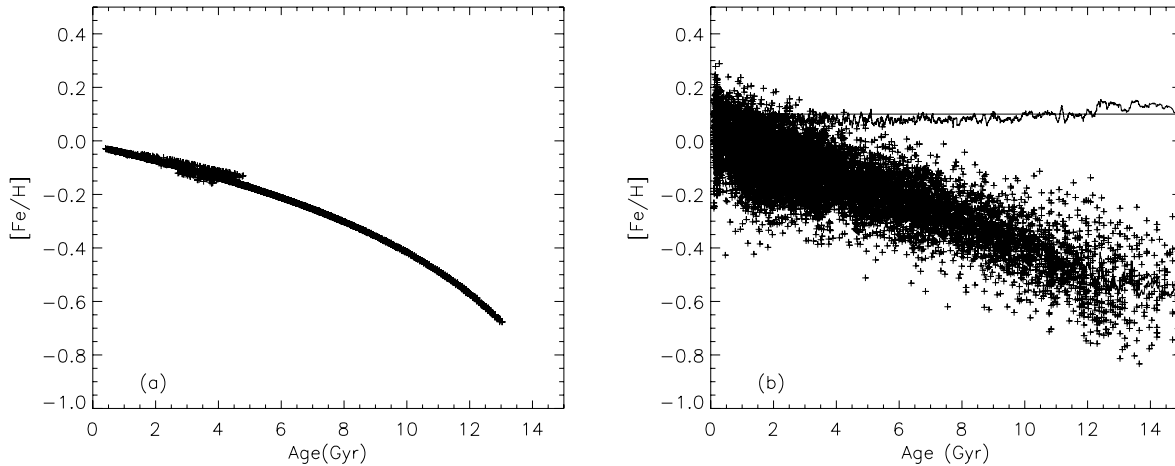


Figure 5. (a) The adopted age–metallicity relation (AMR) as it is recovered when no biases on metallicity or effective temperature are introduced. The only significant deviation from the original relation happens for stars younger than 5 Gyr, due to the overlap of isochrones in the hook region. (b) The AMR relation recovered assuming 0.1 dex dispersion in metallicity and 50 K in effective temperature. No significant dispersion is added by recovered ages.

3.2 Uncertainties in atmospheric parameters

In order to assess how robust is the determination of the AMD from large Strömgren photometric surveys, we need to examine the determination of atmospheric parameters from photometric indices. In our discussion, we focus on effective temperatures and metallicities, because the errors on these two parameters dominate the final error on age determination.

3.2.1 Effective temperatures

The two studies of Feltzing et al. (2001) and Nordström et al. (2004) used the scale of Alonso et al. (1996) that gives effective temperature as a function of the $b - y$ Strömgren index and metallicity. On the temperature range between 5250 and 6250 K, where most datable stars are found, and for ≈ 700 stars in common, the temperatures of Nordström et al. are 136 K lower than the spectroscopic temperatures of Valenti & Fischer (2005). Valenti & Fischer have 94-K difference with Allende Prieto et al. (2004), who also based their temperature scale on that of Alonso et al. (1996). Luck & Heiter noted a difference of 158 K between their spectroscopic scale and that of Allende Prieto et al. (2004). Santos, Israelian & Mayor (2004) have noted also an offset of 139 K in the same sense between their spectroscopic determinations and the temperature scale of Alonso et al. (1996), and similar results are also found in Takeda et al. (2005). Ramírez & Meléndez (2005a) revised the scale of Alonso et al. (1996) to produce essentially the same scale. There seems to be a real dichotomy of the order of 100–150 K between the photometric and spectroscopic effective temperature scales, and we take the view that this is the amount of possible systematic errors on effective temperatures. In order to know which scale is correct, we need an independent estimator of the effective temperatures. This can be provided by effective temperatures derived from the Stefan–Boltzmann relation, measurements of stellar angular diameters and bolometric fluxes, or a scale based on such basic data. This is provided, for example, by Di Benedetto (1998), which gives a $T_{\text{eff}}-V-K$ relation calibrated on effective temperatures derived from angular diameters. We have cross-correlated the effective temperatures from the catalogue of Di Benedetto (1998) with those from the GCS catalogue and found 190 common stars with $B - V$ between 0.3 and

1.0. The differences in effective temperatures between the two scales are plotted in Fig. 7(a), and confirm that, in the crucial range $B - V = 0.5-0.7$, Nordström et al. (2004) underestimated effective temperature by ≈ 100 K. Fig. 7(b) shows the difference between the spectroscopic temperatures of Valenti & Fischer (2005) and those of the GCS catalogue for 740 objects. The discrepancies are very similar, in extent and amplitude, to those of Di Benedetto (1998). We have estimated a mean correction to apply to the GCS effective temperatures by fitting a polynomial to the joint data sets of Di Benedetto (1998) and Valenti & Fischer (2005). This fit is shown in Fig. 7(b).

3.2.2 Metallicities

Discrepancies in the metallicity of solar neighbourhood dwarfs (Section 2) illustrate the difficulties of adopting a correct photometric metallicity scale. Establishing a calibration of photometric metallicities meets several difficulties, one of which is the systematic differences between various spectroscopic data sets. Although there are several possible causes for mismatch between spectroscopic scales, it is known that effective temperature differences of about 100 K induce an offset of about 0.06–0.07 dex. This is an obvious possible explanation for the differences between the data sets of Valenti & Fischer (2005) and Allende Prieto et al. (2004). A second problem is biases that depend on colour, which are usually not seen by visualizing simple correlations between spectroscopic metallicities and photometric estimates. It is crucial that such biases be eliminated, because they would easily affect the shape of the AMD, since colour on the main sequence is strongly correlated with age.

It has been shown that such biases operate in the Strömgren calibration of metallicity from Schuster & Nissen (1989) for G and F dwarfs (Haywood 2002), although the bias may not be detected in simple spectroscopic–photometric metallicity correlations. This bias is difficult to correct, and it is not eliminated from the sample of Nordström et al. (2004), although the authors claimed to have proceeded to new adjustments. A general underestimate of the metallicity is apparent in Nordström et al. (2004) when their catalogue is compared with spectroscopic metallicities. For example, there is a mean difference of -0.075 dex with Valenti & Fischer (2005) (834 stars). A similar offset is observed with the compilation

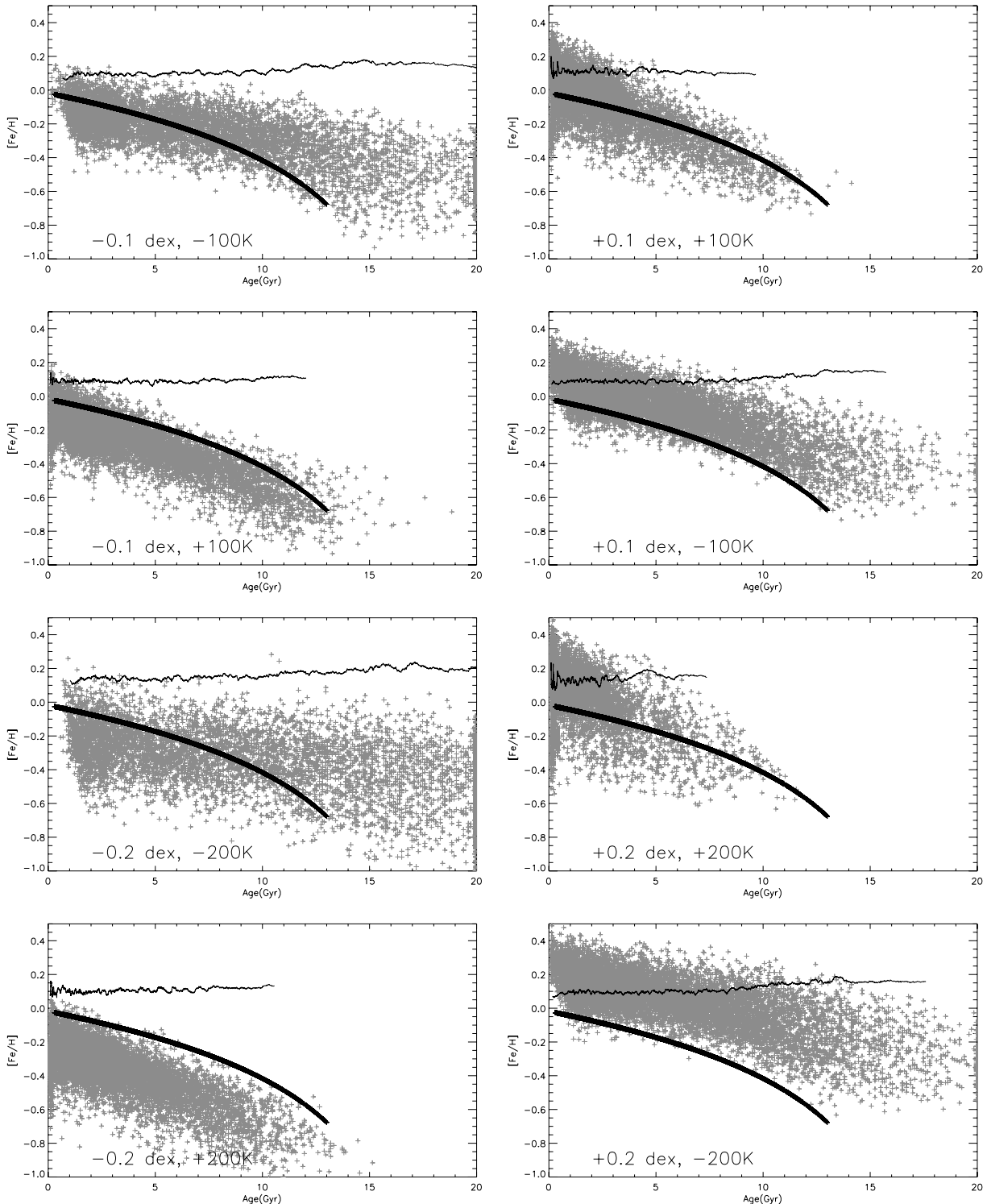


Figure 6. Theoretical age–metallicity relation (thick curve), and samples of about 10 000 ‘stars’ whose ages have been recovered assuming the various systematic biases given in each plot. We also assume Gaussian random errors on metallicities of 0.1 dex, and 50 K on temperatures. The thin curve in each plot is the metallicity dispersion calculated over 100 points.

of Cayrel de Strobel et al. (2001), varying from -0.06 between $0.4 < B - V < 0.5$, to zero above this limit. These are general values, but a detailed comparison reveals more problematic differences.

Fig. 8(a) shows the $(B - V, [Fe/H])$ distribution from Nordström et al. (2004) for field stars, together with their metallicities for the

Hyades stars. It is known that the spectroscopic metallicity of the Hyades stars is usually measured between 0.10 and 0.14 dex, as indicated by the two horizontal lines in the plot. It is remarkable that, in the interval where most of the datable stars are found ($B - V < 0.6$), the metallicity of the Hyades stars from Nordström et al. is underestimated by 0.15–0.2 dex. Although this problem could

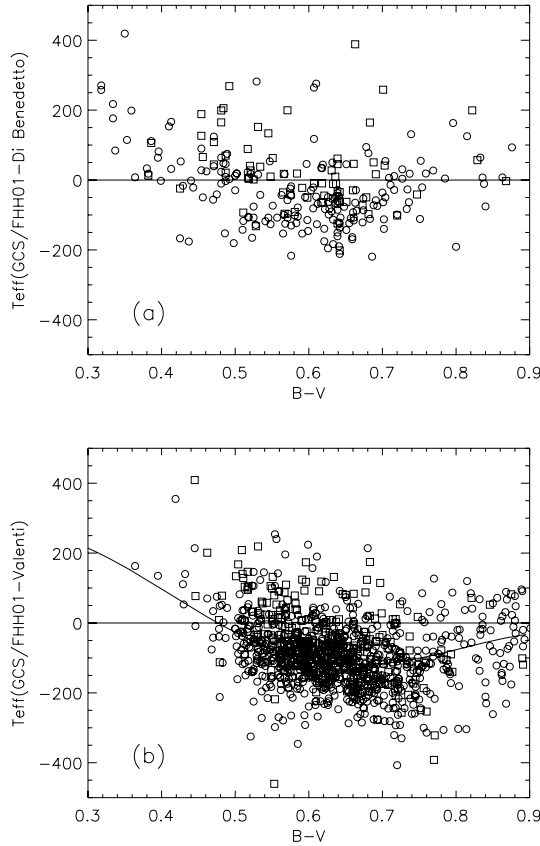


Figure 7. (a) Differences between effective temperatures from the GCS and the catalogue of Di Benedetto (1998) (circles), for 179 stars with $0.3 < B - V < 0.9$ and Feltzing et al. (2001) for 70 common objects (squares). (b) 740 stars within the same limits from Valenti & Fischer (2005). The curve is a fit to the combination of the two data sets. It is used for correcting the effective temperatures in the GCS catalogue.

affect only the cluster members, the similar wavy behaviour of the field star distribution and the Hyades stars leaves little doubts that the problem is general in the catalogue and indicates serious colour effects in the metallicity calibration.

This is confirmed by Figs 9(a) and (b), which shows the $(B - V, [Fe/H])$ distribution obtained with two, independent but consistent, metallicity scales. The first one is a set of stars with $[Fe/H]$ derived from Geneva photometry [using metallicity calibration from Haywood (2001) and Geneva photometric indices, it is designated hereafter as ‘Geneva metallicities’], and the second is made of spectroscopic metallicities from various sources (Balachandran 1990; Edvardsson et al. 1993; Gratton, Carretta & Castelli 1996; Favata, Micela & Sciortino 1997; Feltzing & Gustafsson 1998; Chen et al. 2000; Fulbright 2000; Bensby, Feltzing & Lundström 2003; Erspamer & North 2003; Takeda et al. 2005; Valenti & Fischer 2005; Woolf & Wallerstein 2005). These two distributions are very similar, although the spectroscopic one is clearly incomplete. Considering that the $B - V$ scale is also an age sequence, with older stars being progressively included towards higher $B - V$, they present the following characteristics. The range of metallicities is clearly much narrower for blue, or young, objects. This is due not only to the (expected) appearance of metal-poor, but also to more metal-rich objects at redder colour. It is apparent that for the youngest (bluest) objects, the upper metallicity is approximately that of the Hyades cluster (star symbols in Fig. 9a). This implies that the progressive

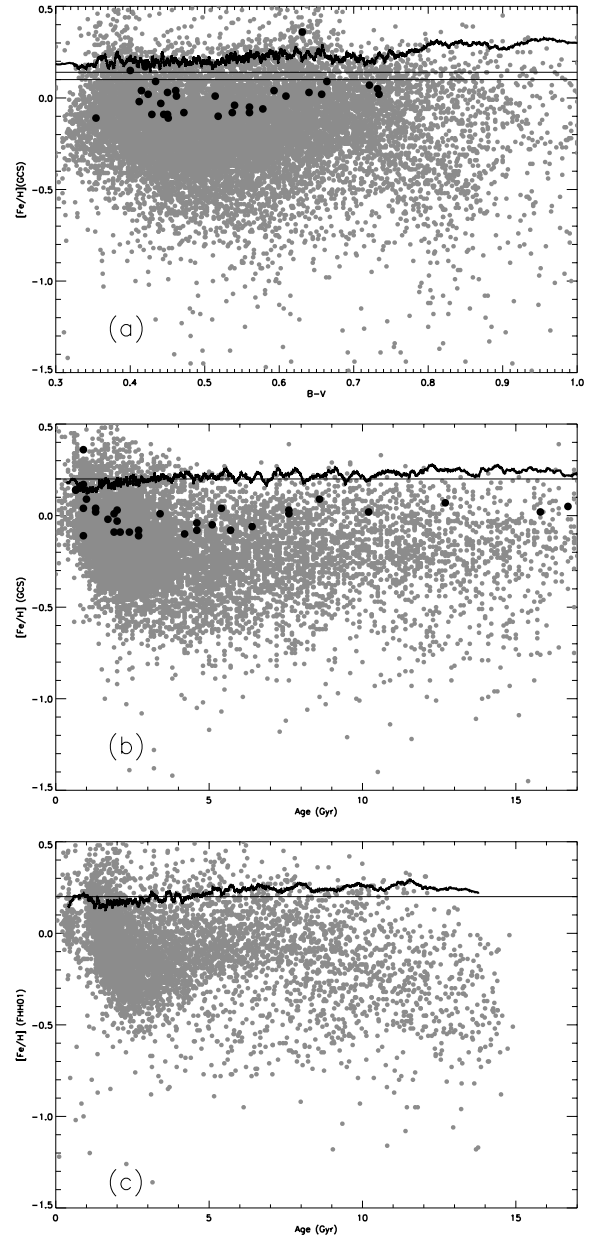


Figure 8. (a) $(B - V, [Fe/H])$ data from the catalogue of Nordström et al. (2004). The two horizontal lines bracket the measured spectroscopic metallicity of the Hyades cluster (0.1–0.14 dex), while the dots are the Hyades stars from the catalogue of Nordström et al. The thick curve is the metallicity dispersion calculated over 100 points. (b) The AMDs for field stars and the Hyades stars from the GCS catalogue. The wavy pattern seen in (a) is also reflected in the AMD (b). An inspection of the ages of individual Hyades stars in the catalogue shows that they correlate with $B - V$. The thick curve is the metallicity dispersion calculated over 100 points. The thin horizontal line is a guide to evaluate the dispersion. (c) The AMD for field stars from Feltzing et al. (2001). Patterns in the AMDs, (b) and (c), are a combination of a defective metallicity calibration, the ‘terminal age bias’ and systematics in the temperature scale.

increase in the upper metallicity towards greater $B - V$ in the sample is due to the inclusion of progressively older stars, starting from the Hyades metallicity at +0.15 dex and reaching +0.5 dex. This can be evaluated visually with the curve of turn-off points at different metallicities for a 5-Gyr isochrone. We comment further on this point in Section 4. The second feature of importance is the fact

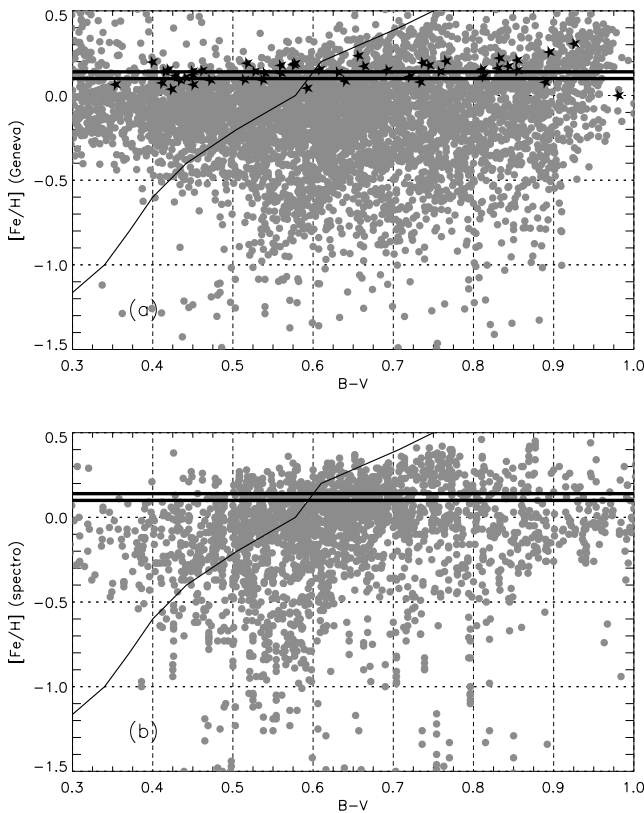


Figure 9. (a) $(B - V, [Fe/H])$ distribution using Geneva photometric metallicities (about 5100 stars). The thick horizontal lines bracket the spectroscopy metallicity of the Hyades (0.10–0.14 dex). The star symbols show the metallicity of the Hyades stars according to the Geneva photometry. The thin line gives the turn-off $B - V$ colour as a function of metallicity for a 5-Gyr isochrone. (b) $(B - V, [Fe/H])$ for spectroscopic metallicities from various sources. The similarities between the two figures contrast with the differences with the data from Nordström et al. (2004) (Fig. 8a). Note, in particular, the metal-rich stars at $B - V > 0.7$, absent from Nordström et al. (2004). The wavy structure seen in Fig. 8(a) is not seen either.

that the youngest objects do show a significantly narrower range of metallicities than the redder, and, in the mean, older, objects. Note that (1) this feature is robust, since it is independent of any age determination, and (2) it is contradicting the recurrent claim of a uniform dispersion at all ages that have been claimed in most recent studies of the AMD, and certainly points to a problem in the determination of ages. In Section 4 of this paper, it is shown that new ages, based on revised atmospheric parameters, are consistent with the $(B - V, [Fe/H])$ relation.

There are two distinct features that are easily seen when comparing these $(B - V, [Fe/H])$ data sets with those of Nordström et al. (2004). The first one is the wavy behaviour seen in Nordström et al. which is absent in the other metallicity samples. The second is the near-absence of cold ($B - V > 0.65$), super-metal-rich ($[Fe/H] > 0.2$ dex) stars in the GCS that are conspicuous in Geneva photometric metallicity, and whose gradual appearance is clearly visible in the spectroscopic data (Fig. 9b). (The small uprise of metallicities seen in Nordström et al. data at $0.60 < B - V < 0.65$ is due to biased metallicities, as will be shown later in this section.) This is mainly a sampling problem: 16 per cent of the sample have $B - V > 0.65$ and $[Fe/H] > 0.2$ dex in Valenti & Fischer (2005) and the Geneva samples, 4 per cent in Nordström et al. Isochrones show that at $[Fe/H] = 0.3$ dex and age > 5 Gyr, turn-off stars have $B - V > 0.67$. There are

17 stars in the GCS catalogue within these limits, and the same number in Valenti & Fischer (2005), although it is more than 10 times smaller. Out of these 17 objects, only two have a GCS age greater than 5 Gyr. In view of these numbers, the scarcity of stars at $[Fe/H] > 0.2$ dex and 4–5 Gyr in the AMD from Nordström et al. (2004) is more likely to be a selection effect than real depletion. This should be emphasized, since the authors insist that their age–metallicity coverage is complete.

3.3 The age distribution of Feltzing et al. (2001) and Nordström et al. (2004)

Comparison between the AMDs of Feltzing et al. (2001) and Nordström et al. (2004) (Fig. 8) shows that more or less sophisticated dating methods do not lead to drastically different results. Although the error analysis is certainly different, the general characteristics of the AMDs are the same in the two studies. These are: (1) a decrease in the mean metallicity with decreasing age between 10 and 5 Gyr, (2) a clump of stars at age < 3 Gyr, (3) the existence of young (age < 5 Gyr) metal-poor ($[Fe/H] < -0.5$ dex) stars and, correlatively, the relative depletion of old metal-poor objects, and (4) a high dispersion at all ages. We comment on each of these features in turn.

3.3.1 Decreasing metallicity with age

The AMD of Nordström et al. (2004), as well as the one of Feltzing et al. (2001), shows a mean decrease in the metallicity between 8–10 Gyr and 4–5 Gyr, before a sharp rise at younger ages (Figs 8b and c). A similar decrease is seen in the $(B - V, [Fe/H])$ distribution of Nordström et al. (2004) (Fig. 8a), between $B - V = 0.7$ and 0.5. This feature is reproduced identically on the Hyades stars (black dots), so that it is most probably due to a defective metallicity calibration. The similarity between the ‘wavy’ pattern of the colour and age metallicity distributions is obvious, and shows that the AMD reflects mainly metallicity variations that are visible in the $(B - V, [Fe/H])$ plot. Note that the interesting matter here is the fact that the age–metallicity pattern of the Hyades stars reflects the field star sample. The large errors on individual ages of the Hyades stars are less surprising, since these are near the zero-age main-sequence, and therefore particularly sensitive to errors on the metallicities and effective temperatures. The cluster stars confirm that the metallicity variations in age closely follow those seen as a function of $B - V$. The decrease in the metallicity of the Hyades stars with age between 9 and 5 Gyr strongly suggests that the similar apparent decrease in field stars is only reflecting the same defect in the metallicity calibration.

3.3.2 The clump of stars at age < 3 Gyr

The most conspicuous pattern in the AMDs of Nordström et al. and Feltzing et al., is the ‘clump’ of stars at age < 3 Gyr, spanning more than 1 dex in metallicity, from $[Fe/H] < -0.5$ to $[Fe/H] \approx 0.5$. Is this feature real? The sudden rise of the Hyades metallicity from -0.1 to 0.2 dex within 2 Gyr, closely following that of field stars, suggests that it is not. It suggests that the youngest field stars have overestimated metallicities, while those at age 2–3 Gyr have underestimated metallicities. We first focus on the young, metal-rich objects.

(i) Overestimated metallicities.

Nordström et al. (2004) suggested that the super-metal-rich young stars in the GCS catalogue could, in part, be giant stars misleadingly

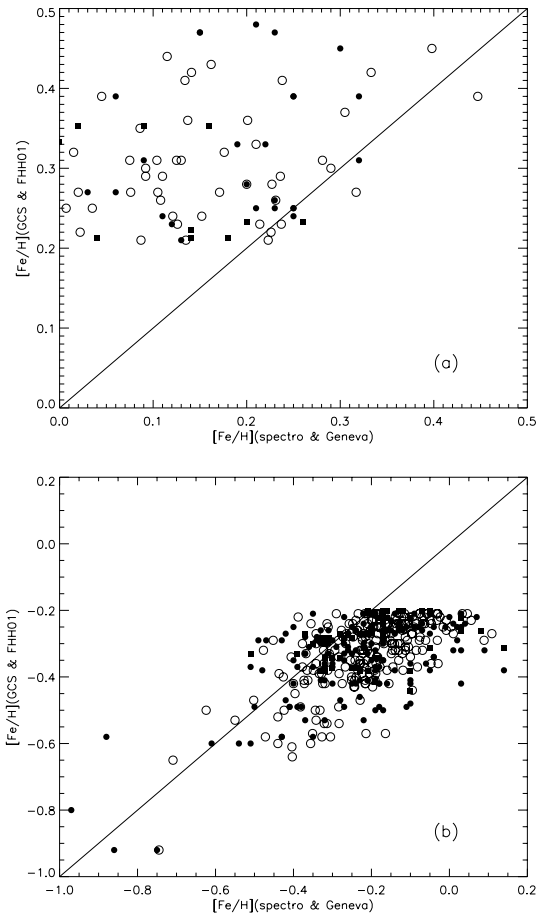


Figure 10. (a) Spectroscopic data vs stars that have $[\text{Fe}/\text{H}] > 0.2$ dex and age < 3 Gyr in Nordström et al. (2004, GCS catalogue) (dots) and Feltzing et al. (2001) (filled squares). When available, Geneva photometric metallicities (discussed in Section 3.2.2) versus Nordström et al. (2004) metallicities have also been plotted (open circles), showing the same trend. (b) Stars that have $[\text{Fe}/\text{H}] < -0.2$ dex and age < 3 Gyr in Nordström et al. (2004) and Feltzing et al. (2001). The symbols are the same as in (a).

included due to improper dereddening. However, half of the stars with $[\text{Fe}/\text{H}] > 0.25$ dex and age < 3 Gyr in their catalogue have a parallax greater than 10 mas and are unlikely to suffer from important reddening problems. The other half is made of objects whose absolute magnitude and colour show that they are evolved main-sequence or subgiant stars. While problems in reddening correction may be a valid explanation for these stars, it remains speculative. Comparison with spectroscopic metallicities suggests another explanation by showing that they have overestimated metallicities. Stars selected in the GCS with $[\text{Fe}/\text{H}] > +0.2$ dex and age < 3 Gyr have been compared with spectroscopic values from the catalogues of Cayrel de Strobel et al. (2001), Feltzing & Gustafsson (1998) and Valenti & Fischer (2005), in Fig. 10. Although only 26 objects (eight in Feltzing et al. 2001) have been found, this is sufficient to confirm that photometric metallicities are overestimated. All 26 objects are either main-sequence or subgiant stars within 100 pc, most at nearer than 70 pc, so that reddening problems are excluded. Note that all measurements available for a given star in Cayrel de Strobel et al. (2001) are plotted in these figures. In addition, the GCS catalogue has been correlated, for the same selections, with the sample of Geneva photometric metallicities discussed in Sec-

tion 3.2.2. Thirty-eight stars were found, and are plotted as open circles in Fig. 10, showing the same trend as the spectroscopic data.

(ii) Underestimated metallicities.

At 2–3 Gyr, the Hyades stars suggest that metallicities in Nordström et al. and Feltzing et al. are probably underestimated. Again, the confirmation comes from spectroscopic determinations, as can be checked in Fig. 10(b): stars selected in the catalogue of Nordström et al. with $[\text{Fe}/\text{H}] < -0.2$ dex and age < 3 Gyr are compared with spectroscopic values from the catalogue of Cayrel de Strobel et al. (2001). There are 78 objects in common between the two data sets [24 for the data set of Feltzing et al. (2001)]. Fig. 10 shows all values available for each object in the catalogue of Cayrel de Strobel et al. (2001), and demonstrates the underestimate with no ambiguity.

Together with errors on effective temperatures, the two biases described here are sufficient to stretch the metallicities and produce the salient clump in the two AMDs of Nordström et al. (2004) and Feltzing et al. (2001). After having corrected these defects, it is shown in Section 4 that stars at $[\text{Fe}/\text{H}] < 3$ Gyr have a metallicity in continuity with older stars, and do not form a specific pattern.

3.3.3 Young metal-poor stars

Inspection of Fig. 8(b) shows that, at medium to low metallicities in the GCS catalogue, young stars are more numerous than old stars. There are 522 stars with $[\text{Fe}/\text{H}] < -0.4$ and age > 6 Gyr, but 829 with age smaller than this limit. At $[\text{Fe}/\text{H}] < -0.6$ (fully in the thick-disc regime), ‘old’ stars (as just defined) are the majority, but there are, however, 45 per cent of ‘young’ objects. If the limit is shifted to 9 Gyr, this percentage rises to 72 per cent. Although these stars represent a minor subset of the whole catalogue, they are essential to characterize the AMD of Nordström et al. (2004), since they give the impression that old stars are not particularly deficient stars. The characteristics of these stars show that they can be classified in two categories. The first category is made of the youngest stars (age < 3 Gyr) which mostly have $B - V < 0.5$, and whose metallicity is underestimated. These were studied in the previous section. Note that, among this subsample, a few stars at $B - V < 0.5$ are probably genuinely young, with metallicities that are truly deficient relatively to their age. This is confirmed for objects which have spectroscopic metallicities, such as HIP 116082, 32851, 47048 or 83243. These are discussed further below. The second category is the group of cold objects ($B - V > 0.75$). There are 73 such objects with measured ages and $[\text{Fe}/\text{H}] < -0.4$ dex in the GCS catalogue, 51 with age younger than 7 Gyr. These are mostly stars at the beginning of the red giant branch. For this peculiar subsample, the few objects in common with the catalogue of Cayrel de Strobel et al. (2001) do not show significant systematics in effective temperature or metallicity. When compared with the isochrone of Girardi et al. (2000) (used by Nordström et al. 2004), it can be verified that these objects are correctly fitted by old isochrones (10–12 Gyr) with intermediate metallicities, see Fig. 11, although they are several Gyr younger in Nordström et al. (2004). However, in this metallicity range, Nordström et al. have shifted stellar models by ≈ -0.011 dex in $\log T_{\text{eff}}$, because of a known discrepancy between model and *main-sequence* data in this metallicity range (Lebreton 2000). There is no evidence that this discrepancy also concerns the base of the red giant branch. At $M_V = 2.8$ –3.0, typical of these objects, the difference in $\log(T_{\text{eff}})$ between a 7- and 11-Gyr isochrone is 0.01 dex (see Fig. 11), the amount of the temperature correction applied by Nordström et al. (2004). Shifting models to lower temperatures is

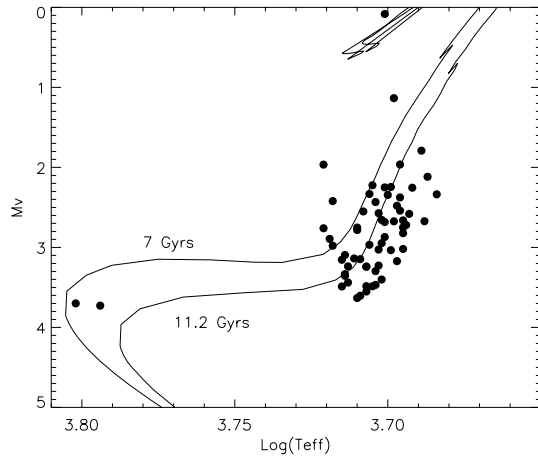


Figure 11. Stars in GCS catalogue with age < 9 Gyr, $[\text{Fe}/\text{H}] < -0.4$ and $B - V > 0.75$. The 2 isochrones are from Girardi et al. (2000) and have ages of 7 and 11.2 Gyr, $Z = 0.004$. In Nordström et al., models at this metallicity have been shifted by 0.01–0.015 dex in $\log(T_{\text{eff}})$ because of problems in main-sequence effective temperatures. However, the visible consequence is that stars at the base of the red giant branch will be more coincident with a 7-Gyr or younger isochrone. Comparison of these stars with the $(M_V, B - V)$ fiducial sequence of 47 Tuc shows they are genuinely old.

equivalent to shifting observed stars towards higher temperatures, producing the effect that is seen in Fig. 6, or creating young, metal-poor objects. Therefore, it is not surprising that the majority of these stars are found at rather young ages in the GCS catalogue, while the old metal-poor region is correlatively depleted. Comparison between the positions of the fiducial sequence of 47 Tuc and these stars in the HR diagram confirms that they are old objects.

3.3.4 The scatter in the age–metallicity relation

Under- and over-estimated metallicities in Nordström et al. (2004) and Feltzing et al. (2001) (see Fig. 10) stretch the AMD by at least ± 0.1 – 0.2 dex at ages < 3 Gyr. Fig. 6 (simulated biases) shows that, over the same age interval, combining these two biases scatters the metallicities from about -0.4 to $+0.4$ dex when effective temperatures are overestimated, and from -0.6 to $+0.4$ dex when they are underestimated, even though we started from a monotonic age–metallicity relation with zero dispersion. We show in the next section that, with revised ages, the dispersion at < 3 Gyr is most probably about 0.1 dex, which can mostly be attributed to the observational scatter in photometric metallicities.

Simulated biases show that underestimated effective temperatures uniformly populate the AMD between $-0.6 < [\text{Fe}/\text{H}] < 0.0$ dex at all ages, increasing the rms dispersion to 0.2 dex for the oldest stars. Given the fact that our simulated biases are oversimplistic, that many effects have not been taken into account (we assumed no intrinsic cosmic scatter), that our model age–metallicity relation is probably overestimating the change of metallicity, we see it as a normal consequence that a uniform scatter in the AMD has been found from photometric surveys, even though the real intrinsic cosmic scatter could be as small as the one measured in the local ISM, on meteoritic pre-solar dust grains, or on element ratios (that is < 0.04 dex).

In any case, we emphasize that the $(B - V, [\text{Fe}/\text{H}])$ plots (Fig. 9) show unambiguously that the cosmic scatter increases towards redder, hence older, stars. This, and the above arguments, strongly

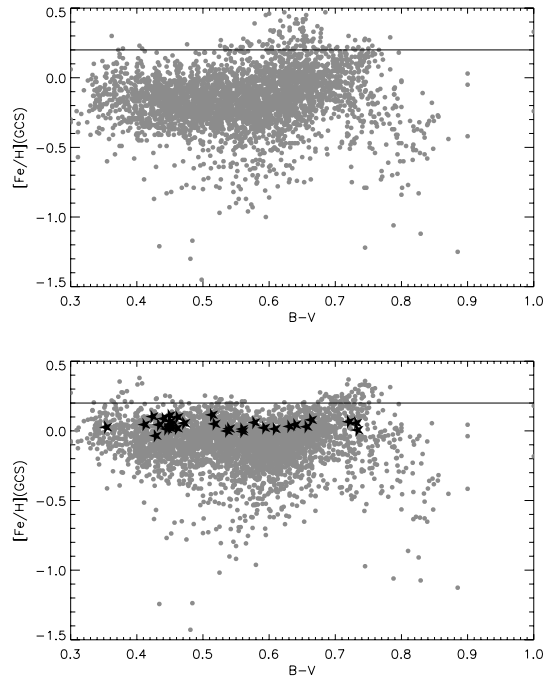


Figure 12. (a) $(B - V, [\text{Fe}/\text{H}])$ for a subsample of the GCS catalogue, selected as described in the text. (b) $(B - V, [\text{Fe}/\text{H}])$ for these same stars with metallicity derived as described in the text.

suggest that the large scatter in metallicity *at all ages*² found in Nordström et al. (2004) and Feltzing et al. (2001), is not real.

4 A REVISED AGE–METALLICITY DISTRIBUTION

In order to illustrate the sensitivity of the final AMD to initial inputs (metallicities, temperatures), we now recalculate the AMD with modified effective temperatures and different metallicities. Following our comments in Section 3.2.1, we first correct the effective temperatures of Nordström et al. according to the correction calculated in Fig. 7. Although that will reduce or eliminate the systematic shift in temperature, the observational dispersion will (obviously) remain. Reducing the random dispersion on effective temperatures would imply different strategies and data and is beyond the scope of this paper.

Correcting the metallicities given in the two cited studies is difficult because of the complex intrication of the different biases with $B - V$ colour and Strömgren indices. The simplest procedure is to adopt another similar metallicity calibration, which shows significant improvement over those used by Nordström et al. or Feltzing et al. We have used the calibration given by Ramírez & Meléndez (2005a) which is of similar form as the one given by Schuster & Nissen (1989), but seems to be well behaved in a $(B - V, [\text{Fe}/\text{H}])$ plot (Fig. 12). Note, however, that a small colour term in the sense that $[\text{Fe}/\text{H}]$ decreases with $B - V$ (seen in the Hyades stars as well as in field stars) has been corrected as follows;

² We suggest hereafter, Section 4, that the distribution of metallicities at a given age is probably the combination of two components, one with a small dispersion, and the other with greater dispersion, made of stars that migrated to the solar neighbourhood; the importance of this component should increase with age.

$[\text{Fe}/\text{H}] = [\text{Fe}/\text{H}]_{\text{RM}} - 0.5(B - V) + 0.35$ for stars bluer than $B - V = 0.7$. The calibration has been applied to the stars that have $b - y$, m_1 , c_1 indices in Olsen (1993) and Olsen (1994), and a parallax in the *Hipparcos* catalogue with relative error less than 10 per cent (or distance less than ~ 100 pc), in order to minimize reddening effects. Olsen (1983) has not been used, because comparison with the two other data sets showed significant inconsistencies which contribute to the dispersion in metallicities. No correction for reddening was adopted. In case a star was found in the two catalogues, the mean of the two determinations was adopted. This selection yields 4469 stars for which $(B - V, [\text{Fe}/\text{H}])$ is plotted in Fig. 12(a), with metallicities from the GCS catalogue, while plot (b) shows the new metallicities. We note, in passing, that the general form of these two plots is similar to that of the Geneva sample (Fig. 9a), and different from that of Fig. 8(a). The main differences between Figs 12(a) and (b) are (1) the absence of the metallicity uprise between $B - V = 0.6$ and 0.7 and $[\text{Fe}/\text{H}] > +0.2$ dex in (b), which was due to overestimated values in the GCS catalogue, and (2) the substantially lower metallicities at $B - V < 0.6$, also present in the calibration of Ramírez & Meléndez (2005a), and that was corrected as explained previously.

About 3650 objects in this sample have an age in the GCS catalogue. The AMD for the GCS catalogue for these stars is given in Fig. 13(a), and although it is a subsample, it retains all the main characteristics of the AMD of the GCS catalogue. Fig. 13(b) has been obtained from the same parameters (T_{eff} , $[\text{Fe}/\text{H}]$), but with ages derived with the method employed in our study and the isochrones of Yi et al. (2003). It illustrates that changing the dating method and isochrones does not change significantly the shape of the AMD, although it must be noted that most of the young metal-poor stars in the GCS catalogue selection are shifted towards older ages. This is illustrated, in particular, by the thick-disc stars (star symbols, see below for a discussion of these objects). Fig. 13(c) shows the AMD for the same stars with age redetermined using the Yi et al. (2003) isochrones and corrected effective temperatures and metallicities. The circle symbols show the new ages and metallicities for the Hyades stars. Compared to the GCS catalogue parameters for the Hyades, metallicities are nearer to the expected metallicity of this cluster, and are independent of $B - V$ (within the uncertainties). Obviously, the derivation of ages is still not optimal and still affected by significant errors. This is not surprising, since we have not optimized the derivation of either effective temperatures or metallicities.

There is, however, a clear indication that the newly derived ages and metallicities are superior to those from the GCS catalogue. This is seen by comparing the dispersion in metallicity as a function of $B - V$ (Fig. 12) and age (Fig. 13) for the two data sets. If there is an (even loose) relation between age and metallicity, it is expected that the dispersion in metallicity be lower when correlated with age, because $B - V$ is only representing a mean age sequence. However, in the case of the GCS catalogue, the dispersion is larger at ages < 4 Gyr [0.16–0.19 dex, Fig. 13(a)] than in $B - V$ (for $B - V < 0.47$, Fig. 12a) (0.14–0.16 dex), whereas in our case, the dispersions are 0.10–0.11 (Fig. 13c) and 0.13–0.16 dex (Fig. 12b) over the same intervals.

Interestingly, the AMD we obtain with our new age and metallicity determinations is quite different from those of Nordström et al. (2004) and Feltzing et al. (2001), and we now give a detailed account of the differences.

(i) Three of the characteristics previously discussed (the clump; young, intermediate metallicity stars; decrease in metallicity between 10 and 5 Gyr) are now absent. The overall dispersion varies

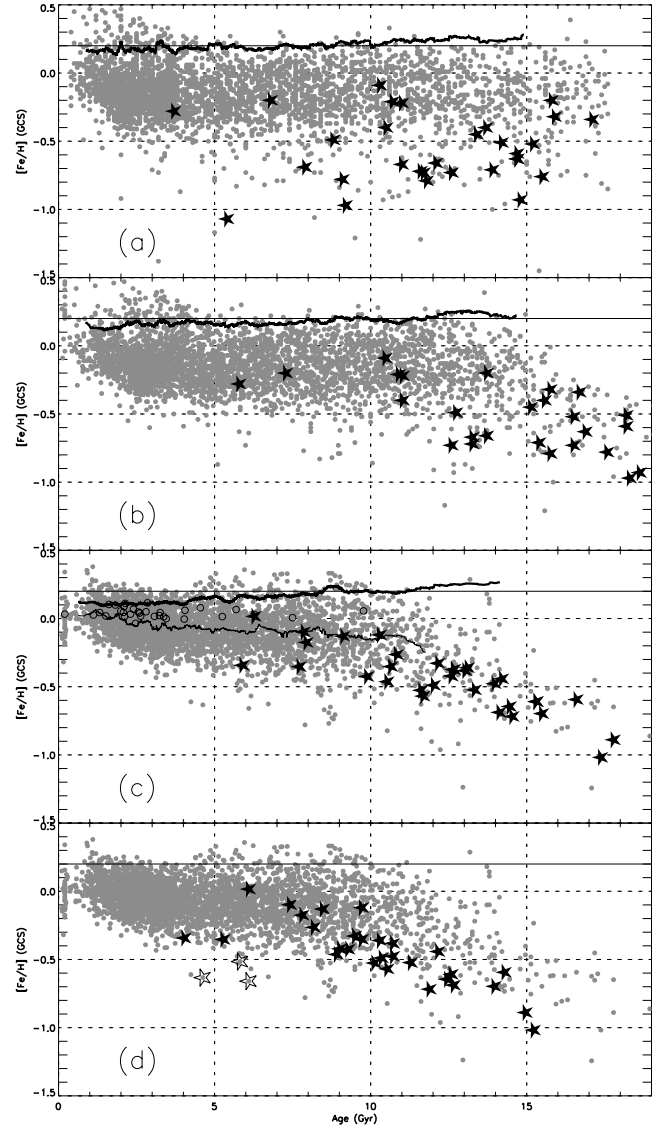


Figure 13. AMD for various age and metallicity determinations. The horizontal line at $[\text{Fe}/\text{H}] = 0.2$ dex is given to ease the comparison. The thick curve on the first three plots is the dispersion in metallicity calculated over 300 points. The solid stars in all plots are thick-disc stars according to their kinematics (see the text). (a) The AMD according to the subsample of the GCS catalogue, for stars selected as detailed in the text. Ages and metallicities are all from the GCS catalogue. (b) The AMD for the same stars, with the atmospheric parameters from the GCS catalogue, but with ages derived from the Yi et al. (2003) isochrones. The α -element content was set to 0 for all stars. (c) AMD for the same sample, but derived from the new $[\text{Fe}/\text{H}]$ (see the text), effective temperatures from the GCS corrected as described in the text, and using the isochrones of Yi et al. (2003). The α -element content was set to 0 for all stars. The open circles are the new ages derived for the Hyades stars. The thin lower curve is the mean metallicity calculated over 100 points. (d) Same as (c), except that the ages of thick-disc stars (solid stars) have been derived taking into account the α -element content according to the value listed in Soubiran & Girard (2005). The open stars are objects with $[\text{Fe}/\text{H}] < -0.4$ from Soubiran & Girard (2005), flagged as disc stars according to their kinematics and α -element content.

from below 0.11 dex at age < 3 Gyr to more than 0.22 dex at ages > 10 Gyr. There is a significant difference with the dispersion measured on the data of Nordström et al. (2004) in Fig. 13(a), which is about 0.17 dex at ages of < 3 Gyr. Interestingly, a dispersion of

0.1 dex is about what is expected from measurement uncertainty, which means that intrinsic scatter at ages <3 Gyr is compatible, within the uncertainties, with the one measured on abundances in the ISM and isotopic ratios of meteoritic pre-solar dust grains (≈ 0.04 dex, Cartledge et al. 2006; Nittler 2005).

(ii) The increase in the metallicity range towards super-metal-rich objects at ages greater than 4–5 Gyr corresponds to a similar increase in the $(B - V, [\text{Fe}/\text{H}])$ plot at $B - V > 0.6$ (Fig. 12, the same is also observed with Geneva and spectroscopic metallicities, Fig. 9). This feature, which is seen neither in Nordström et al. (2004) nor in Feltzing et al. (2001), shows the inclusion in the solar neighbourhood of objects that are gradually older and more metal rich. The $(B - V, [\text{Fe}/\text{H}])$ plot of the Geneva sample shows that these objects reach $[\text{Fe}/\text{H}] = +0.5$ dex at 5 Gyr. The extent of these features at $B - V > 0.8$ in this last sample suggests that the absence of stars older than 9–10 Gyr in Fig. 13(c) is probably a selection effect of the Strömgren sample (the turn-off colour of a 10-Gyr isochrone at $[\text{Fe}/\text{H}] = 0.3$ dex is $B - V = 0.75$).

The sample of Geneva metallicities $(B - V, [\text{Fe}/\text{H}])$ in Fig. 9(a) shows that local young objects ($B - V < 0.4$) reach a maximum metallicity similar to that of the Hyades cluster ($[\text{Fe}/\text{H}] = 0.10$ – 0.15 dex). If the origin of the stars more metal rich than this limit is radial migration (Grenon 1999), and given an estimate of the radial metallicity gradient, it could, in principle, be feasible to measure an upper limit to the rate of radial migration. However, the radial gradient is uncertain, with values between 0.04 and 0.1 dex kpc^{-1} , implying a maximum rate of migration loosely constrained between 1.75 and 0.7 kpc Gyr^{-1} .

(iii) There is a similar extension of the lower metallicity interval that intervenes at ages >4 Gyr. For only three of these objects, an α abundance ratio could be found (open star symbols in Fig. 13d), showing with no ambiguity that these are bona fide thin-disc stars. Pont & Eyer (2004) have commented on young, metal-poor stars in Edvardsson et al. (1993), explaining that these objects were unlikely to be truly young, since none had a measured mass (from fitting the HR position with an isochrone) greater than $1.1 M_{\odot}$. We emphasize that unlike the stars studied by Pont & Eyer (2004), all these three objects have an estimated mass higher than this limit. Also, given their scarcity (seven objects with $[\text{Fe}/\text{H}] < -0.5$ dex and age <7 Gyr out of 3650 stars in our sample), it is unsurprising that the Edvardsson et al. (1993) sample contains none of these objects. We note that these metal-poor ‘young’ candidates seem to appear at a similar age as metal-rich objects, although statistically more significant samples are needed, and this can be attributable to a similar cause (radial migration), but from the outer disc.

(iv) The median value calculated in (overlapping) subsamples of 200 points between 10 Gyr and the youngest stars shows that the increase in metallicity between the two limits is of the order of -0.15 dex, with a small upturn at age <3 Gyr. There is a change of slope when shifting from the thin to the thick disc, for which the metallicity increases by about 0.5 dex within 5 Gyr.

(v) As a final test to the effect of our corrections on the atmospheric parameters, we selected stars that are known to belong to the thick disc according to their kinematics. We have cross-correlated our sample with the compilation of stars published by Soubiran & Girard (2005), which yielded 29 stars. These 29 stars are shown in all four plots of Fig. 13 as solid star symbols. The most remarkable result is seen when comparing the different age distributions. In the first case [plot (a), GCS catalogue], no particular trend is seen, and the spread of points illustrates our comments on the various biases (see the previous section). Part of this spread is reduced with the ages derived from the isochrones of Yi et al. (2003), due to the fact

that no correction to the effective temperature scale of the models has been applied; hence, we avoid the bias detailed in Section 3.3.3, which generates young metal-poor stars. The new ages calculated with the corrected atmospheric parameters (Fig. 13c) show a clear, distinct trend of increasing metallicity with decreasing age, and confirms the existence of an age–metallicity relation within the thick disc proposed by Bensby, Feltzing & Lundström (2004). In this case, we have neglected the α -element content and set $[\alpha/\text{Fe}] = 0.0$ dex. Finally, in Fig. 13(d), we use the value of α -element content listed in Soubiran & Girard (2005) for each star to compute the isochrones and derive the ages. The correlation obtained is even better than that in the previous plot (c).

5 DISCUSSION

We reviewed the metallicity distribution of stars in the solar neighbourhood, published in the recent years and found that recent spectroscopic data sets show good agreement with our own finding (Haywood 2001), with a peak at $[\text{Fe}/\text{H}] = -0.05$. Using scale-height corrections based on a σ_w – $[\text{Fe}/\text{H}]$ relation derived from a sample of solar neighbourhood stars, we arrive at the conclusion that there is no deficit of metal-poor stars relative to the closed-box model. The low-metallicity part ($[\text{Fe}/\text{H}] < -0.5$ dex) of our relation being dominated by thick-disc stars, this conclusion is valid only if the thick-disc stars are genuine disc stars, not of extragalactic origin. It is also in agreement with expectations from simple arguments of Galactic structure. Standard chemical evolution models usually acknowledge the existence of a thick disc as a genuine Galactic population, but its contribution to the local solar radius metallicity distribution is often undervalued. On the other hand, looking at the metallicity distributions recently published, we find the contribution of stars, having the metallicity of the thick disc, to be generally incompatible with simple Galactic structure constraints.

Despite the recent detailed analysis of large photometric Strömgren data sets, it appears that published AMDs are essentially reflecting noise in the determination of atmospheric parameters and derived ages. Significant improvement should come from reducing systematic biases in the determination of metallicity and effective temperatures from photometric indices. A first step in this direction is made here, and shows a limited increase in the mean metallicity of the thin disc, superposed on another, steeper relation in the thick disc. This scheme confirms that the disc has endured most of its chemical evolution during the thick-disc phase, and has remained (chemically) unchanged since then.

In the last 3 Gyr, the measured dispersion in metallicity is 0.10–0.11 dex, compatible with error measurements, and implying a small scatter of the young disc population. After 3 Gyr, the progressive appearance of a metal-rich population reaching $[\text{Fe}/\text{H}] \approx +0.5$ dex at ages greater than 5 Gyr is established. It is suggested that these super-metal-rich stars are the contaminant objects resulting from radial migration from the inner disc. A similar spread at lower metallicity is seen at approximately the same age, giving stars reaching $[\text{Fe}/\text{H}] \approx -0.7$ at 5 Gyr, attributable to an equivalent migration from the outer disc. These characteristics are consistent with the $(B - V, [\text{Fe}/\text{H}])$ distribution presented in Section 3, which, although independent of any age determination, is a source of information on the AMD. Note also that the metallicity scale of the $(B - V, [\text{Fe}/\text{H}])$ distribution is independent of the Strömgren metallicity scale used in the derivation of ages. If this general picture is correct, we expect that the metallicity distribution at age greater than 3 Gyr is a superposition of a narrow (about 0.05 dex or less) distribution of stars born at solar radius and a broader distribution of stars that have

moved to the solar radius. We note that the metallicity distribution of Fuhrmann (2004, figs 49 and 50) presents such characteristics, with clearly a superposition of 2 Gaussians with dispersions of about 0.05 and 0.25 dex centred on solar metallicity.

Altogether, these elements point to a picture where chemical and dynamical evolution lead to structured, if complex, patterns of age and metallicity, but not a general, structureless, dispersion. It is apparent that, in the level of abundance reached by the Galaxy prior to the thin-disc formation as well as in the shape of the local metallicity distribution, the thick disc must have played a central role. This is now discussed.

5.1 The thick disc: is there a continuity argument?

Is there a continuity argument to invoke when discussing the origin of the thick disc? An inspection of α -element ratios versus metallicity plots (see e.g. Pritzl, Venn & Irwin 2005; Reddy, Lambert & Allende Prieto 2006) suggests the following.

(i) The halo presents no evidence of having been enriched by Type Ia supernovae (SNeIa) (even when allowing for a generous threshold in galactocentric rotational velocity at about $+100$ – 120 km s^{-1} , see fig. 2 in Pritzl et al. 2005). There have been suggestions that low $[\alpha/Fe]$ implied contamination by SNeIa. However, most recent studies (Arnone et al. 2005, and references therein) indicate that halo stars seem to have a higher level of homogeneity in element ratios $[X/Fe]$ than that previously thought (<0.06 dex), with levels of $[\alpha/Fe]$ compatible with no contamination by SNeIa.

(ii) While there is a clearly visible increase in the $[\alpha/Fe]$ ratio towards low-metallicity stars of the thin disc ($[\alpha/Fe] = 0.1$ – 0.2 dex at about $[Fe/H] \approx -0.5$ – 0.7 dex, see Reddy et al. 2006, fig. 12), there is no evidence that the thin disc has escaped contamination by SNeIa.

(iii) In the solar neighbourhood at least, the thick disc seems to be the *only* population that shows both enrichment phases by SNeII and SNeII + SNeIa, suggesting that the thick disc could be a transition population between the halo and thin disc. The suggestion is made stronger if one realizes that an extragalactic thick disc would require that an accreted satellite has just the right (α/Fe , Fe/H) pattern to meet the halo on one side and the thin disc on the other. As a matter of fact, there is no detected chemical or kinematical discontinuity between the ‘rotating halo’ and thick disc (see Gratton et al. 2003) so far. If the small dispersion of abundance ratios measured on halo stars is confirmed, then the continuity between enrichment levels in the different elements between the halo and the thick disc should become a stringent constraint for the origin of this last population. For example, Nissen et al. (1994) measured $[Mg/Fe] = 0.41$ with an rms dispersion of <0.06 dex on halo stars with $-3.2 < [Fe/H] < -1.8$, while Reddy et al. (2006, and references therein) measured thick-disc stars to have a similar rms dispersion and $[Mg/Fe]$ comparable with that of Nissen et al. (1994) at $[Fe/H] < -0.8$ dex. Confirmation on a larger scale is needed, but it suggests that the ‘rotating halo’ and the thick disc may be the same population.

There is, however, an observed discontinuity between the thin and thick discs, with the (α/Fe , Fe/H) sequence of the two being almost parallel. It has been proposed that since the most metal-rich stars in the thick disc have a higher metallicity than the most metal-poor stars in the thin disc, there has been a dilution of metals by an infall episode in the temporal gap between the two populations (Bensby et al. 2005; Reddy et al. 2006). The AMD of the previous section shows that metal-poor disc stars are not specifically old for their

metallicity, a characteristic that is not expected if it is assumed that the first thin-disc stars had formed after the infall episode at $[Fe/H] \approx -0.6$ dex. Moreover, the AMD of Fig. 13 shows that the mean metallicity of old disc stars is nearer to $[Fe/H] = -0.2$ dex than -0.6 dex, a fact which does not fit well with the dilution scenario above. A perhaps more convenient explanation is that metal-poor thin-disc stars found in local samples have been moved to the solar neighbourhood by radial migration from outside the solar circle. This scenario, suggested by our conclusions that the AMD has been shaped by radial migration, is also well in agreement with the results presented by Carney et al. (2005) and Yong, Carney & de Almeida (2005). These authors presented evidence, from open clusters, field giants and cepheids, that the mean disc metallicity decreases to $(-0.4, -0.6)$ dex at $R_{GC} = 10$ – 11 kpc. An even more interesting clue found by these authors is that the $[\alpha/Fe]$ ratios of these stars reach about $+0.1$ to $+0.2$ dex. These are just the characteristics of the most metal-poor thin-disc stars in the solar neighbourhood sample, which also show this slight increase in $[\alpha/Fe]$. Finally, we note that Carney et al. (2005) and Yong et al. (2005) found that the gradient in metallicity and $[\alpha/Fe]$ flattens beyond $R_{GC} = 10$ – 11 kpc, which may explain why the metal-poor thin-disc stars found in local samples are limited to about $[Fe/H] \approx -0.6$ dex. Taking these considerations into account, it might then be expected that the thin disc starts forming its stars (at solar galactocentric radius) not at -0.6 dex, but at a higher metallicity which Fig. 13 suggests might be around -0.2 dex, or above. This is also consistent with the ($[\alpha/Fe]$, $[Fe/H]$) plot in Reddy et al. (2006), which, showing excellently the separation between the thin and thick discs, also shows that the tip of the metal-rich thick disc is around $(-0.3, -0.2)$ dex.

This leaves the possibility that there is a gap in $[\alpha/Fe]$ between the thin disc and thick disc (Pagel 2001) of the order of $+0.05$ dex, consistent with a temporal gap between the two populations. A jump in $[\alpha/Fe]$ with no significant variation in the general metal content (<0.1 dex) does not require exchange of gas (inflow or outflow) but simply that star formation ceased for a period of time sufficiently long that the ISM was enriched in iron by SNeIa for $[\alpha/Fe]$ to decrease by 0.05 dex.

5.2 Life without the ‘G dwarf problem’

In view of what has just been said about the thick disc, how do we interpret the fit between the dwarf metallicity distribution and the closed-box model? We cannot eliminate the option that the thick disc is an accreted population, since there is by now no clear-cut evidence against this solution. In this eventuality, however, we note that the metallicity distribution would then have to be limited to ‘pure’ thin-disc, solar radius stars. Limiting the sample to objects born within a restricted range around this radius would probably make the metallicity much thinner than the one derived in Haywood (2001) – probably less than 0.1 dex dispersion. Casuso & Beckman (2004) have explicitly considered that the thick disc should not be part of the metallicity distribution, although not formally considering the thick disc as a population of extragalactic origin. Their conclusion that infall should be an increasing function of time, is not surprising.

In the case that the thick disc is a genuine Galactic population, the disc (thin + thick) metallicity distribution is not in marked disagreement with the closed-box model. The problem is reminiscent of the discussion about the metallicity distribution function (MDF) of the halo. According to predictions of hierarchical clustering in Λ cold dark matter (Λ CDM) cosmologies, the stellar halo is supposed

to be an archetypal open system, formed from many independent units. However, the observed MDF of the halo is shown to be fitted reasonably well by a simple box model distribution (Oey 2003) over a large range of metallicities. More generally, it is apparent that the closed-box model gives a good fit to the MDF of spheroids for most of the metallicity interval. There is often a problem in fitting the metal-poor tail of these distributions, but this concerns a small fraction of the stars, and is not comparable with the local disc ‘G dwarf problem’. The question, however, remains: why does the closed-box model provide an honest fit to these systems? The question for the disc MDF is more or less the same. The exact profile of the low-metallicity tail of the thick disc is unknown, but globally, the simple model provides a fair fit to the observed distribution. Because discs are now conceived as open systems that build up continuously from accreted gas, this result is not expected. We emphasized that, strictly speaking, our result only means that the alleged mismatch between the observed MDF and the simple model cannot be used as an argument for infall models. It does not imply that infall is not a crucial ingredient in models, although it strongly suggests that standard infall models should be revised. We note that first results from chemodynamical models (Brook et al. 2005) are encouraging. In particular, Brook et al. (2005) have come quite close to reproducing the characteristics of the distinct (α -element) chemical signatures of the thin and thick discs, with the thick disc formed during a merging phase of gas-rich ‘building block’, whereas the thin disc forms inside-out, at a more quiescent epoch, from continuously accreting gas. The interesting point is given by an inspection of the metallicity distribution of the (thin + thick) disc generated by their model (Martel et al. 2006, their fig. 3), which shows it is quite similar to a closed-box model distribution. This suggests that although the local data are not conclusive indication for prolonged infall, as classically proposed, a metallicity distribution with the simple model characteristics is neither an indication of a closed system.³ Said differently, the simple model may have lost its paradigmatic strength.

ACKNOWLEDGMENTS

I would like to thank the referee for the very helpful comments and suggestions which much improved the first version of this paper.

REFERENCES

- Alibés A., Labay J., Canal R., 2001, *A&A*, 370, 1103
 Allende Prieto C., Barklem P. S., Lambert D. L., Cunha K., 2004, *A&A*, 420, 183
 Alonso A., Arribas S., Martínez-Roger C., 1996, *A&AS*, 117, 227
 Arnone E., Ryan S. G., Argast D., Norris J. E., Beers T. C., 2005, *A&A*, 430, 507
 Balachandran S., 1990, *ApJ*, 354, 310
 Bensby T., Feltzing S., Lundström I., 2003, *A&A*, 410, 527
 Bensby T., Feltzing S., Lundström I., 2004, *A&A*, 421, 969
 Bensby T., Feltzing S., Lundström I., Ilyin I., 2005, *A&A*, 433, 185
 Brook C. B., Gibson B. K., Martel H., Kawata D., 2005, *ApJ*, 630, 298

³ Ironically though, it may be noted that at least two hypotheses of the simple model are little disputed, and one fact is hard to prove wrong: that the initial mass function is constant with time, that the ISM is well mixed and, with the present results, that the solar neighbourhood metallicity distribution is like a closed-box model distribution.

- Carlberg R. G., Dawson P. C., Hsu T., Vandenberg D. A., 1985, *ApJ*, 294, 674
 Carney B. W., Yong D., de Almeida M. L. T., Seitzer P., 2005, *AJ*, 130, 1111
 Cartledge S. I. B., Lauroesch J. T., Meyer D. M., Sofia U. J., 2006, *ApJ*, 641, 327
 Casuso E., Beckman J. E., 2004, *A&A*, 419, 181
 Cayrel de Strobel G., Soubiran C., Ralite N., 2001, *A&A*, 373, 159
 Chen Y. Q., Nissen P. E., Zhao G., Zhang H. W., Benoni T., 2000, *A&AS*, 141, 491
 Chiappini C., Matteucci F., Gratton R., 1997, *ApJ*, 477, 765
 de Bruijne J. H. J., Hoogerwerf R., de Zeeuw P. T., 2001, *A&A*, 367, 111
 Di Benedetto G. P., 1998, *A&A*, 339, 858
 Edvardsson B., Andersen J., Gustafsson B., Lambert D. L., Nissen P. E., Tomkin J., 1993, *A&A*, 275, 101
 Erspamer D., North P., 2003, *A&A*, 398, 1121
 Favata F., Micela G., Sciortino S., 1997, *A&A*, 323, 809
 Feltzing S., Gustafsson B., 1998, *A&AS*, 129, 237
 Feltzing S., Holmberg J., Hurley J. R., 2001, *A&A*, 377, 911
 Fuhrmann K., 2004, *AN*, 325, 3
 Fulbright J. P., 2000, *AJ*, 120, 1841
 Garnett D. R., Kobulnicky H. A., 2000, *ApJ*, 532, 1192
 Girardi L., Bressan A., Bertelli G., Chiosi C., 2000, *A&AS*, 141, 371
 Gratton R. G., Carretta E., Castellì F., 1996, *A&A*, 314, 191
 Gratton R. G., Carretta E., Desidera S., Lucatello S., Mazzei P., Barbieri M., 2003, *A&A*, 406, 131
 Grenon M., 1999, *Ap&SS*, 265, 331
 Haywood M., 2001, *MNRAS*, 325, 1365
 Haywood M., 2002, *MNRAS*, 337, 151
 Hearnshaw J. B., 1972, *Mem. RAS*, 77, 55
 Israelian G., Santos N. C., Mayor M., Rebolo R., 2004, *A&A*, 414, 601
 Jørgensen B. R., 2000, *A&A*, 363, 947
 Kotoneva E., Flynn C., Jimenez R., 2002a, *MNRAS*, 335, 1157
 Kotoneva E., Flynn C., Chiappini C., Matteucci F., 2002b, *MNRAS*, 336, 879
 Kovtyukh V. V., Soubiran C., Belik S. I., 2004, *A&A*, 427, 933
 Laws C., Gonzalez G., Walker K. M., Tyagi S., Dodsworth J., Snider K., Suntzeff N. B., 2003, *AJ*, 125, 2664
 Lebreton Y., 2000, *A&A*, 350, 587
 Luck R. E., Heiter U., 2005, *AJ*, 129, 1063
 Martel H., Brook C., McGee S., Gibson B., Kawata D., 2006, in Sutantyo W., Premadi P. W., Mahasena P., Hidayat T., Mineshige S., eds, *Proc. 9th Asian-Pacific Regional IAU Meeting*. Institut Teknologi Bandung Press, Bandung, West Java.
 Ng Y. K., Bertelli G., 1998, *A&A*, 329, 943
 Nissen P. E., Gustafsson B., Edvardsson B., Gilmore G., 1994, *A&A*, 285, 440
 Nittler L. R., 2005, *ApJ*, 618, 281
 Nordström B. et al., 2004, *A&A*, 418, 989
 Oey S. M., 2003, *MNRAS*, 339, 849
 Olsen E. H., 1983, *A&AS*, 54, 55
 Olsen E. H., 1993, *A&AS*, 102, 89
 Olsen E. H., 1994, *A&AS*, 106, 257
 Pagel B. E. J., 1989, in Beckman J. E., Pagel B. E. J., eds, *Evolutionary Phenomena in Galaxies*. Cambridge Univ. Press, Cambridge, p. 201
 Pagel B. E. J., 2001, in Vangioni-Flam E., Ferlet R., Lemoine M., eds, *Cosmic Evolution*. World Scientific Press, Singapore, p. 223
 Pont F., Eyer L., 2004, *MNRAS*, 351, 487
 Powell A., 1972, *MNRAS*, 155, 483
 Pritzl B. J., Venn K. A., Irwin M., 2005, *AJ*, 130, 2140
 Ramírez I., Meléndez J., 2005a, *ApJ*, 626, 446
 Ramírez I., Meléndez J., 2005b, *ApJ*, 626, 465
 Reddy B. E., Lambert D. L., Allende Prieto C., 2006, *MNRAS*, 367, 1329
 Renda A., Kawata D., Fenner Y., Gibson B. K., 2005, *MNRAS*, 356, 1071
 Rocha-Pinto H. J., Maciel W. J., 1996, *MNRAS*, 279, 447
 Rocha-Pinto H. J., Maciel W. J., 1997, *A&A*, 325, 523
 Rocha-Pinto H. J., Scalo J., Maciel W. J., Flynn C., 2000, *ApJ*, 531, L115

Romano D., Chiappini C., Matteucci F., Tosi M., 2005, *A&A*, 430, 491
Santos N. C., Israelian G., Mayor M., 2004, *A&A*, 415, 1153
Schuster W. J., Nissen P. E., 1989, *A&A*, 221, 65
Sommer-Larsen J., 1991, *MNRAS*, 249, 368
Soubiran C., Girard P., 2005, *A&A*, 438, 139
Takeda Y., Ohkubo M., Sato B., Kambe E., Sadakane K., 2005, *PASJ*, 57,
27
Taylor B. J., Croxall K., 2005, *MNRAS*, 357, 967
Tinsley B. M., 1974, *ApJ*, 192, 629
Twarog B. A., 1980, *ApJ*, 242, 242

Twarog B. A., Anthony-Twarog B. J., Tanner D., 2002, *AJ*, 123, 2715
Valenti J. A., Fischer D. A., 2005, *ApJS*, 159, 141
Woolf V. M., Wallerstein G., 2005, *MNRAS*, 356, 963
Wyse R. F. G., Gilmore G., 1995, *AJ*, 110, 2771
Yi S. K., Kim Y.-C., Demarque P., 2003, *ApJS*, 144, 259
Yong D., Carney B. W., de Almeida M. L. T., 2005, *AJ*, 130, 597

This paper has been typeset from a $\text{\TeX}/\text{\LaTeX}$ file prepared by the author.